DEVELOPMENT OF MODEL FOR LARGE-BORE ENGINE COOLING SYSTEMS

by

CLINT EDWARD KENDRICK

B.S., Kansas State University, 2009
B.S., Washburn University, 2009

A THESIS

submitted in partial fulfillment of the requirements for the degree

MASTER OF SCIENCE

Department of Mechanical and Nuclear Engineering
College of Engineering

KANSAS STATE UNIVERSITY
Manhattan, Kansas

2011

Approved by:

Major Professor
Dr. Kirby Chapman

Abstract

The purpose of this thesis is to present on the development and results of the cooling system logic tree and model developed as part of the Pipeline Research Council International, Inc (PRCI) funded project at the Kansas State National Gas Machinery Laboratory. PRCI noticed that many of the legacy engines utilized in the natural gas transmission industry were plagued by cooling system problems.

As such, a need existed to better understand the heat transfer mechanisms from the combusting gases to the cooling water, and then from the cooling water to the environment. To meet this need, a logic tree was developed to provide guidance on how to balance and identify problems within the cooling system and schedule appropriate maintenance.

Utilizing information taken from OEM operating guides, a cooling system model was developed to supplement the logic tree in providing further guidance and understanding of cooling system operation. The cooling system model calculates the heat loads experienced within the engine cooling system, the pressures within the system, and the temperatures exiting the cooling equipment. The cooling system engineering model was developed based upon the fluid dynamics, thermodynamics, and heat transfer experienced by the coolant within the system. The inputs of the model are familiar to the operating companies and include the characteristics of the engine and coolant piping system, coolant chemistry, and engine oil system characteristics. Included in the model are the various components that collectively comprise the engine cooling system, including the water cooling pump, aftercooler, surge tank, fin-fan units, and oil cooler.

The results of the Excel-based model were then compared to available field data to determine the validity of the model. The cooling system model was then used to conduct a parametric investigation of various operating conditions including part vs. full load and engine speed, turbocharger performance, and changes in ambient conditions. The results of this parametric investigation are summarized as charts and tables that are presented as part of this thesis.

Table of Contents

List of Figures

List of Tables

Nomenclature

A list of acronyms, nomenclature, and Greek variables follows.

Acronyms

DR	Daily Temperature Range
DLL	Dynamic Link Library
KSU	Kansas State University
NGML	National Gas Machinery Laboratory
OEM	Original Equipment Manufacturer
PRCI	Pipeline Research Council International
TCV	Thermostatic Control Valve
T-RECS	Turbocharger Reciprocating Engine Computer Simulation
RPM	Revolutions per minute

Nomenclature

A	Area
a	Coefficient of Discretized Equation
B	Bore
b	Constant of Discretized Equation
c	Specific Heat
D	Diameter
f	Friction Factor
g	Gravity
H	Head

h	Convective Heat Transfer Coefficient
K	Piping Friction Factor
k	Thermal Conductivity
ks	Equivalent Sand Grain Roughness
L	Length
M	Mass
$\dot{m}$	Mass Flow Rate
Nu	Nusselt Number
p	Pressure
Pr	Prandtl Number
$\dot{q}$	Heat Transfer Rate
$\ddot{q}$	Heat Flux Rate
R	Thermal Resistivity
Re	Reynolds Number
Sp	Mean Piston Speed
T	Temperature
t	Time
V	Volume
$\dot{V}$	Volumetric Flow Rate
v	Velocity
W	Work Rate
x	Thickness
z	Height

Greek Variables

Δ Change in a condition, as in ΔT is the change in temperature

ε Effectiveness

φ Variable in Discretized Equation

γ Specific Gravity

β Pressure Loss Coefficient

ω Average In-Cylinder Gas Velocity

ρ Density

Acknowledgements

First and foremost I offer my sincerest gratitude to my major professor, Dr. Kirby Chapman, who offered me a graduate research assistant position and has provided knowledge, support, and guidance throughout my thesis and graduate career.

Along with my major professor, I would like to thank Dr. Donald Fenton and Dr. Steve Eckels for their time and willingness to be a part of my supervisory committee. My sincere thanks also goes to Dr. Mohamed Toema for his insightfulness and allowing me to bounce ideas off of him.

A special thanks goes to the Pipeline Research Council International, Inc. (PCRI) for providing financial support for the project upon which this thesis is based. Also, I would like to thank Cameron, Dresser-Rand, El Paso, and Panhandle energy for collecting and providing technical information used in the development of this thesis.

I would like to thank my wife, Angel, for her loving support and tolerating the long hours I spent working at the school. A special thanks goes to my brother, Josh, and sister, Jessica, who have always been an exciting distraction from school and work. I am greatly indebted to my parents, Gary and Brenda, who supported me when I was broke, encouraged me when I was down, and loved me when I was difficult. Without my family, all that I have accomplished would be for nothing.

Finally, I would like to thank God for blessing me with a wonderful family, providing me with the intelligence and persistence to accomplish my goals, and constantly reminding me of all that I do not understand.

Dedication

I dedicate this thesis to my wife, Angel, parents, Gary and Brenda, and my siblings, Josh and Jessica for the encouragement and support they provided during my years of study.

Chapter 1 - Introduction

This thesis is based on the work completed as part of a PCRI funded project through the National Gas Machinery Laboratory at Kansas State University. The focus of this section is to outline the objectives, describe the tasks and deliverables, and briefly explain the physics of a cooling system.

1.1 Objective

The objectives of this study are to: 1) combine the information contained in operating and maintenance guides with information obtained via discussions with former and current OEM engine design engineers to develop cooling system guidelines for a variety of engines; 2) document how the cooling system should operate with particular emphasis on the interactions between the various cooling loads, e.g., oil cooler and turbocharger aftercooler, within the engine system; and 3) utilize the gathered information to develop a cooling system model and logic tree.

1.2 PRCI Project Description

1.2.1 Tasks

The PCRI funded project included six primary tasks:

Task 1: Conduct Literature Review

Assemble a detailed summary of cooling system literature, such as operating and maintenance guides, that provides guidance on cooling system operating limits. The research team used information in the public domain as well as information collected from engineers and technicians who have experience operating cooling systems. The outcome of this task was a collection of tables that provides all available information on cooling system operations. The tables are included in Appendix A.

Task 2: Develop a simplified cooling system engineering model

Using Nusselt number formulations and the previous successful work by Chapman (1987) [1] and Chapman et al. [2] (1988), the team developed a simplified engineering model of a typical cooling system. The research team expected this Excel-based model to provide the framework of the project deliverables and be useable by industry engineers and operators. The inputs and outputs are familiar operating parameters, but the core of the model is based on dimensionless parameters to increase model transportability.

Task 3: Visit sites for further information gathering

The site visits were used to collect operational information and experiences from senior operators as well as actual operating data. During the site visits, the research team collected operating data as the operators varies one or more coolant system operating parameters.

Task 4: Tune Engineering Model

The information and data collected in Task 3 was used to tune the engineering model developed in Task 2. The outcome of this task was an Excel-based engineering model of a cooling system that is tuned for two-stroke large bore engines utilized in the natural gas transmission industry. These engines include:

1. Cooper
    a. V-250/V-275
    b. W-330
    c. GMV
2. Clark
    a. TLA
    b. TCV
    c. HBA
3. Ingersoll-Rand
    a. KVS

Depending on the local station configuration and cooling system capacity, the engineering model can be used to optimize coolant flow rate through the engine, cooling water supply pressure, and cooling water supply temperature.

Task 5: Develop an Optimization Logic Tree

The developed logic tree can be used to optimize engine cooling systems. The logic tree was developed so that it is easily usable by station personnel.

Task 6: Develop a complete set of cooling system guidelines

The cooling system guidelines include:

1. All modeling equations with example calculations to set up a particular cooling system;
2. The cooling system setup logic tree with an appropriate example;
3. The detailed literature and information review developed in Task 1; and
4. A series of examples on how to use the guidelines and Excel-based cooling system optimization model.

The guidelines represented the final report of the PRCI funded project, and were submitted to the committee members for review and comments.

1.2.2 Deliverables

This thesis presents on the development and results of the PRCI funded project. The deliverables for the final phase of the project included:

1. Detailed summary of cooling system literature, such as operating and maintenance guides, that provides guidance on cooling system operating limits;
2. A detailed logic flow chart of actions to optimize engine cooling systems that can be followed by plant personnel;
3. Detailed documentation of interviews and statements from retired or nearly-retired engineers and technicians who have experience with cooling system operation; and
4. Cooling system operating guidelines.

1.3 Cooling system overview

Figures 1.1 and 1.2 show the schematics of the single and two loop, engine cooling systems, respectively, used in the development of the engineering model. These two engine cooling systems were chosen due to their difference in component layout and the fact that the aftercooler is not a component on the single loop engine cooling system. Throughout this thesis, the single loop engine cooling system will be referred to as 'system 1' while the two loop cooling system will be referred to as 'system 2.'

The numbers in Figure 1.1 correspond to the various components that make up system 1 where:

1. Engine
2. Surge Tank
3. Coolant Pump
4. Fin-Fan Heat Exchanger
5. Engine Oil Cooler
6. Thermostatic Control Valve

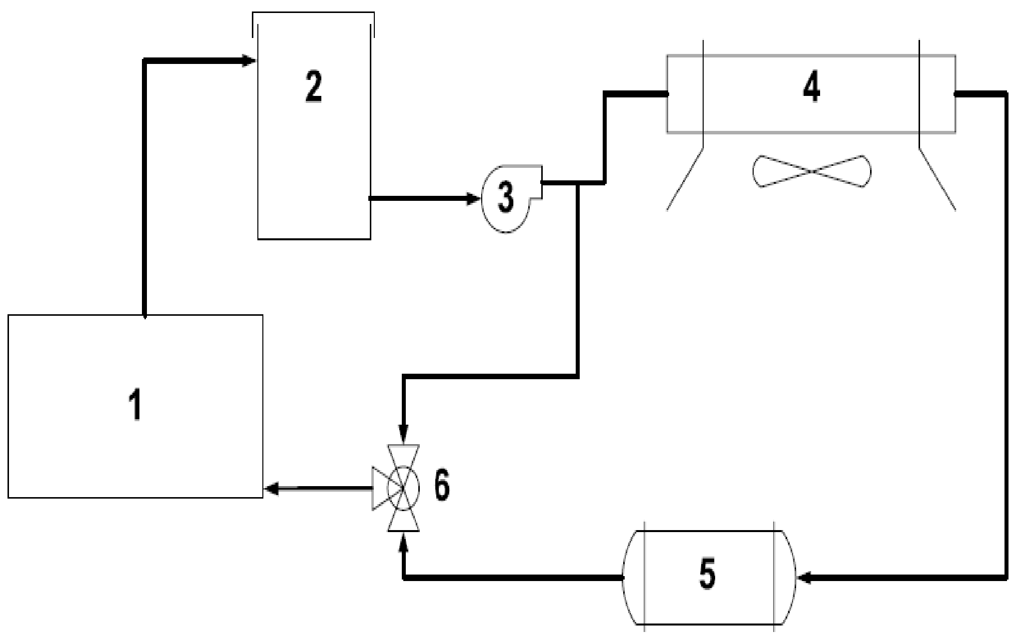

Figure 1.1 – Schematic of single loop cooling system model

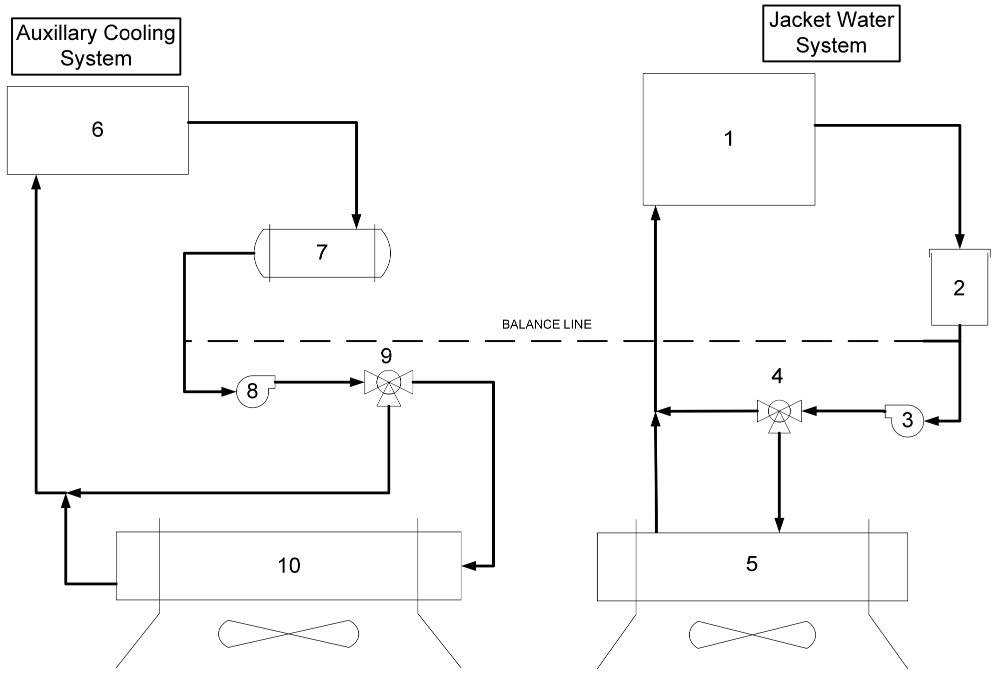

Figure 1.2 – Schematic of dual loop cooling system model

In similar fashion, the numbers in Figure 1.2 correspond to the components that make up system 2 where:

1. Engine
2. Surge Tank
3. Jacket Water Pump
4. Jacket Water Thermostatic Control Valve
5. Jacket Water Fin-Fan Heat Exchanger
6. Aftercooler
7. Engine Oil Cooler
8. Auxiliary Cooling Pump
9. Auxiliary Cooling Thermostatic Control Valve
10. Auxiliary Cooling Fin-Fan Heat Exchanger

Figures 1.1 and 1.2 also illustrate how the coolant circulates through the system with the arrows representing the flow direction.

1.3.1 Energy transfer within cooling system

This section describes the energy transfer and fluid dynamics that occur within the cooling system.

Most of the energy enters the cooling system in the engine according to thermodynamic and heat transfer principles. The primary modes of heat transfer are convection and conduction. Energy is also added to the system in the engine oil cooler and, for system 2, the aftercooler. Energy is removed from the cooling system in the fin-fan unit. The energy added/removed in the engine oil cooler, aftercooler, and fin-fan unit are governed, again, by thermodynamic and heat transfer principles.

1.3.2 Fluid dynamics within coolant piping system

The coolant piping system is comprised of many different components. These components include:

- Piping
- Fittings
- Coolant pump
- Surge Tank
- Cooling Equipment

The coolant circulates from component to component in the piping. The change in height, number of fittings, and length and diameter of the pipe affect the resulting pressure in each section of pipe. The resulting pressure through the piping is governed by fluid dynamic principles.

The coolant pump pressurizes the cooling system and also produces the coolant mass flow rate. The pump head and coolant flow rate are a function of the pump speed which, in turn, is a function of the engine speed.

The surge tank provides the system with room to expand and establish a minimum suction pressure for the coolant pump. The outlet pressure of the surge tank is governed by fluid dynamic principles and depends upon the ambient pressure and the height of the water within the surge tank. For system 2, the surge tank is located on the jacket water side and a balance line connects the two sides at the outlet of the surge tank to the suction side of the auxiliary cooling pump as shown in Figure 1.2. This allows the surge tank to act as an expansion tank for the auxiliary cooling side and provides suction pressure to the auxiliary cooling pump.

The cooling equipment includes the engine, oil cooler, fin-fan unit, and aftercooler. Each component of the cooling system equipment has a corresponding pressure differential that is a function of the coolant mass flow rate. The change in pressure through the cooling equipment is governed by fluid dynamic principles.

Chapter 2 - Literature Review

This section presents a brief review of cooling system design considerations including in-cylinder to coolant heat transfer correlations, incompressible fluid flow, and OEM operating guidelines. Also, a review of various cooling system setups is presented.

2.1 Review of Cooling System Setups

The following collection of literature consists of examples of cooling system setups, including, entire system analysis and precision cooling. The information is valuable in terms of new technology and general cooling system information.

Luptowski et al. [3] presented the work done on the Vehicle Engine Cooling System Simulation (VECSS), developed at Michigan Technological University, enhanced by linking with GT-POWER for the engine/cycle analysis model. Enhanced VECSS (E-VECSS) calculates the effects of cooling system operation on engine performance including accessory power and fuel conversion efficiency. Along with the engine cycle, modeled components include the engine manifolds, turbocharger, radiator, charge-air-cooler, engine oil circuit, oil cooler, cab heater, coolant pump, thermostat, and fan. This tool was then applied to develop and simulate an actively controlled electric cooling system for a 12.7-liter diesel engine.

Robinson et al. [4] performed a review on the achievements and potential of precision engine cooling, along with an extension into nucleate-boiling-based heat transfer. They demonstrated that exploiting the large increases in heat transfer that are possible with nucleate boiling in a controlled manner could lead to lower coolant pressures and lower metal temperatures. This is all achieved with lower coolant flow rates and with a careful avoidance of film boiling. They also stated that evidence suggests nucleate boiling already occurs unintentionally in many engines.

Kays [5] addresses liquid-cooled engines that use atmospheric air as an ultimate heat sink. The author examines various heat exchanger loops that are commonly used for cooling the block, for aftercooling, and for combining block cooling with aftercooling. The mechanisms whereby heat is transferred to the coolant within the engine block, how the heat load is determined, and the implications with regard to surface and fluid temperatures are discussed. The author examines heat exchanger designs that illustrate some of the characteristics of heat exchanger surfaces and the unique features of automotive application.

2.2 Thermal System Modeling

Governing equations developed to model a system are formed from thermodynamic, heat transfer, and fluid dynamic principles. The first law of thermodynamics and the conservation of mass which can be found in any thermodynamic text, such as [6], are:

$$\dot{q} - \dot{W} + \sum \dot{m}_i \left(i_i + \frac{v_i^2}{2} + g z_i \right) - \sum \dot{m}_e \left(i_e + \frac{v_e^2}{2} + g z_e \right) = \frac{dE}{dt} \quad (1)$$

$$\sum \dot{m}_i - \sum \dot{m}_e = \frac{dM_{cv}}{dt} \quad (2)$$

where:

$\dot{q}$ = Heat transfer rate

$\dot{W}$= Work rate

$\dot{m}$= Mass flow rate

i= Enthalpy

v= Velocity

g= Gravity

z= Height

$\frac{dE}{dt}$= Time rate of change of energy

$\frac{dM}{dt}$= Time rate of change of mass

Equations (1) and (2) along with fluid dynamic principles discussed later in Section 2.5 provide the grounds from which a complete thermal system model can be built. This section focuses on methods that can be used to model a complete cooling system and cooling system components.

Stoecker [7] addresses thermal system design through the modeling of thermal equipment and optimization of a system. The author also covers system simulations in which a design can be improved or modified.

Patankar [8] describes the process of converting a non-linear system of equations into a linear system of equations. Each equation in a non-linear system is linearized, or discretized, into the following form:

$$a_e\varphi_e = \sum_i a_i\varphi_i + b_i \tag{3}$$

In this form, the φ's represent the unknowns, the *a*'s are the coefficients of the unknowns, and the *b* terms are constants within the equations. The discretized system of equations still represents the system being modeled and can be solved using an iterative method such as the Gauss-Seidel method.

The Guass-Seidel method, as discussed by Patankar [8], involves calculating the unknowns, φ's, in a certain order and updating the values as the unknowns are calculated. In other words, the value of the φ_i's, in Equation (3), have either already been calculated during the iteration if they occur before φ_e or are the values calculated during the previous iteration.

In terms of heat transfer, the engine cooling system can be represented by a combination of heated flow passages. While the determination of the flow fields and local heat transfer within these complicated flow passages is clearly beyond the scope of this project, the flow passages can be analyzed in terms of the average, but still somewhat local, Nusselt number [9]. The Nusselt number, $N_{u,}$ is a dimensionless heat transfer coefficient defined as:

$$Nu = \frac{hL_c}{k} \tag{4}$$

The term *h* is the convective heat transfer coefficient, the term *Lc* is a characteristic length, and the term *k* is the fluid thermal conductivity. The Nusselt number is further correlated to other operating parameters by a variety of different correlations published in the open literature. One of the most commonly used correlations is the Dittus-Boelter equation [9]:

$$Nu = 0.023Re^{0.8}Pr^{n} \tag{5}$$

The exponent *n* is 0.4 for heating and 0.3 for cooling. The term *Re* is the Reynolds number and the term *Pr* is the Prandtl number. The Reynolds number functionally contains coolant property, flow passage geometry, and flow rate information, and the Prandtl number functionally contains additional coolant property information. Collectively, the Nusselt number contains all information necessary to characterize heat transfer within the flow passages.

The heat exchangers within the engine cooling system can be modeled by methods described by Incropera et al. [9]. A graphical representation of the heat transfer within the heat exchangers is shown in Figure 2.1. Hot and cold fluids enter the heat exchanger. Energy, in the form of heat (illustrated by Q in Figure 2.1), is transferred from the heat fluid to the intermediate metal. Then the energy is transferred from the metal to the cold fluid.

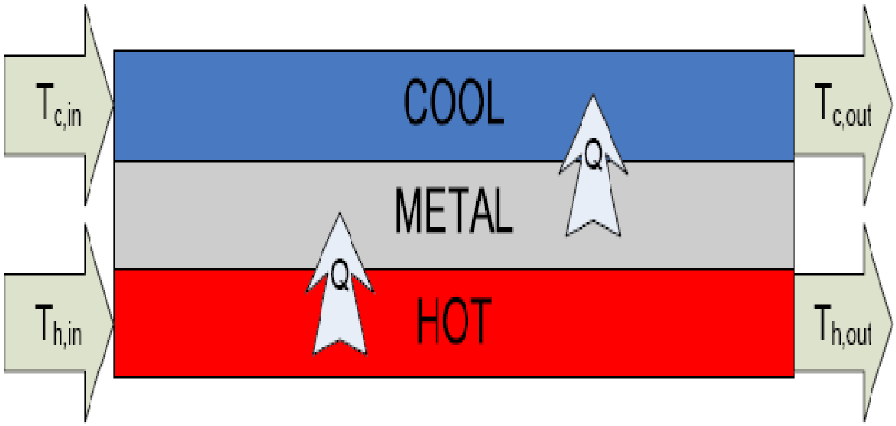

Figure 2.1 – Heat Exchanger Model

The equations that describe the heat exchange process in a heat exchanger, assuming constant specific heat, are:

$$\dot{m}_h c_h \left(T_{h,in} - T_{h,out}\right) - \dot{q}_{h-m} = \frac{d(M_h c_h T_h)}{dt} \tag{6}$$

$$\dot{q}_{h-m} - \dot{q}_{m-c} = \frac{d(M_m c_m T_m)}{dt} \tag{7}$$

$$\dot{m}_c c_c \left(T_{c,in} - T_{c,out}\right) + \dot{q}_{m-c} = \frac{d(M_c c_c T_c)}{dt} \tag{8}$$

In this form, $\dot{m}$ is the mass flow rate, c this the specific heat, T is the temperature, $\dot{q}$ is the heat transfer rate, and M is the mass. The subscript h denotes the hot fluid, c denotes the cooling fluid, and m denotes the intermediate metal. These equations are slightly different for a fin-fan unit due to the fact that the ambient air is the cooling fluid but the same premise applies to all heat exchangers when nucleate boiling is absent.

2.3 Engine Cylinder to Coolant Heat Transfer

The engine cylinder to coolant heat transfer mechanism is where most of the energy enters the coolant within the cooling system. Complex equations are needed to model the in-cylinder heat transfer coefficient. Karamangil et al. [10] developed a model to parametrically determine the convective heat transfer coefficient of a gasoline engine on both the in-cylinder and jacket sides. The combustion products were a function of excess air and fuel. The cylinder temperature and pressure were calculated with a simplistic model based on the First Law of Thermodynamics. The in-cylinder heat transfer coefficient was evaluated using two different expressions; one a specific form of Annand's equation [11] and the other, the Woschni equation [12]. Woschni's equation is expressed as:

$$h_{gas} = 3.26B^{-0.2}p^{0.8}T^{-0.55}w^{0.8} \tag{9}$$

Where h_{gas} is the in-cylinder heat transfer coefficient, B is the bore, p is the pressure, T is the temperature, and w is the average in-cylinder gas velocity. The average in-cylinder gas velocity is characterized by:

$$\omega = C_1\bar{S}_p + C_2\frac{V_dT_r}{p_rV_r}(p - p_m) \tag{10}$$

In this form, C_1 and C_2 are constants, $\bar{S}_p$ is the mean piston speed, V_d is the displacement volume, T_r, p_r, and V_r are the temperature, pressure, and volume of the cylinder with respect to a reference state, p is the instantaneous cylinder pressure, and p_m is the motored cylinder pressure. The constants C_1 and C_2 depend on the period of the engine cycle and the values are typically:

Gas exchange period: C_1=6.18, C_2=0

Compression period: C_1=2.28, C_2=0

Combustion and Expansion period: C_1=2.28, C_2=0.00324

The heat transfer coefficient between the engine block and the cooling water was determined by utilizing Newton's convective heat transfer equation.

The development of the in-cylinder heat transfer coefficient leads into determining the heat flux from the combusting gases to the coolant. Figure 2.2 shows a graphical representation of a piston cylinder setup and the associated heat transfer mechanisms. As shown, combustion occurs within the cylinder and a portion of the energy released during the combustion process is transferred by heat transfer mechanisms through the oil film lining the cylinder, then the cylinder, and lastly to the jacket water circulating around the cylinder.

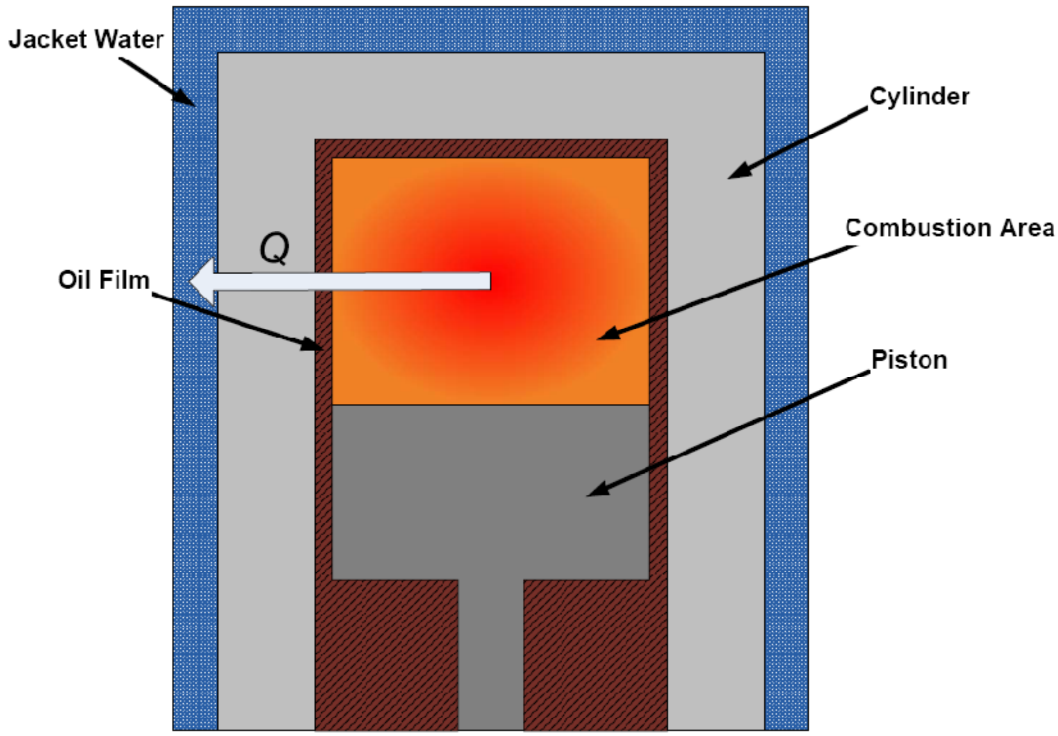

Figure 2.2 - Model of Piston Cylinder Setup

The heat flux from the combustion zone to the jacket water can be determined using thermal resistances as described by Incropera et al. [9]. Figure 2.3 shows a graphical representation of the thermal resistances.

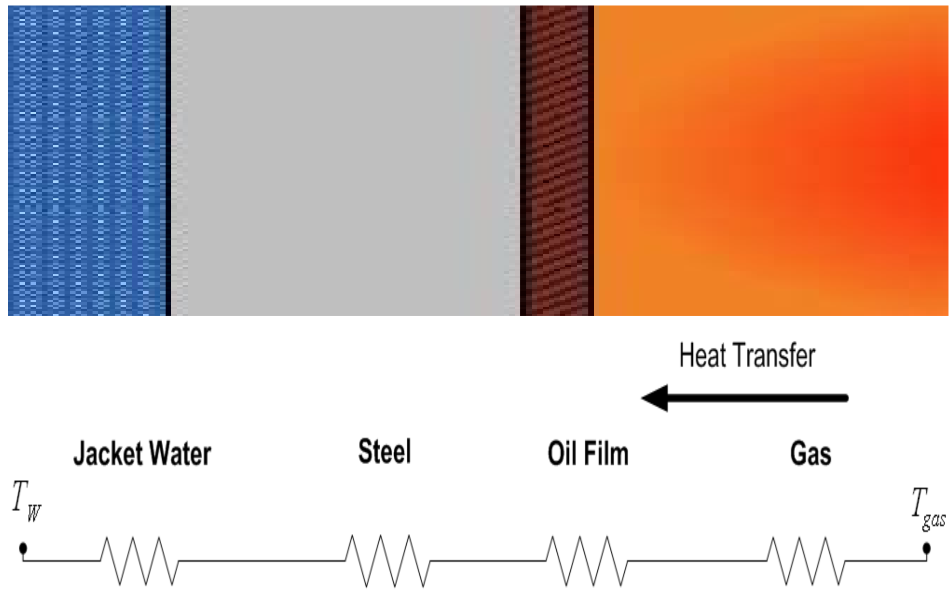

Figure 2.3 – Engine Thermal Resistance Model

The heat flux can then be calculated by using the thermal resistance equations [9]:

$$R_{jw} = \frac{1}{h_{jw}} \tag{11}$$

$$R_{steel} = \frac{x}{k_{steel}} \tag{12}$$

$$R_{oil} = \frac{1}{h_{oil}} \tag{13}$$

$$R_{gas} = \frac{1}{h_{gas}} \tag{14}$$

$$R_{total} = \sum R_i \tag{15}$$

$$\ddot{q} = \frac{T_{gas} - T_{jw}}{R_{total}} \tag{16}$$

Where R is the thermal resistance, h is the convective heat transfer coefficient, k is the thermal conductivity, x is the thickness of the cylinder wall, $\ddot{q}$ is the thermal flux, and T is the temperature. The h_{gas} term represents the in-cylinder convective heat transfer coefficient and can be determined by using Annand's equation [11] or Woschni's equation [12] as previously described.

2.4 Engine Operating Cycle Model

The Turbocharger Reciprocating Engine Computer Simulation program (T-RECS) was developed at the National Gas Machinery Laboratory at Kansas State University. T-RECS applies the first law of thermodynamics for an open system to the cylinder volume for the intake, compression, combustion, expansion, and exhaust processes that in sequence make up the engine operating cycle, allowing for the calculation of the adiabatic flame temperature. During each process, sub models are used to describe geometric features, the thermodynamic properties of the unburned and burned gases, the mass and energy transfers across the system boundary, and the combustion process [13].

Specifically, T-RECS uses a three-zone combustion model, one zone for each of the burned, unburned, and boundary zones. The burning rate can be simulated using either a Wiebe function or a user-entered range for the combustion process. T-RECS also uses the JANAF tables to calculate equilibrium combustion constants [14].

2.5 Incompressible Fluid Flow

An engine cooling system is comprised of many components connected by pipes to form a complete system. Daily and Harleman [15] describe nonuniform flow in conduits and Bernoulli's equation pertaining to pipe flow. The authors also cover head loss and its dimensionless coefficient. They show how to address flow through loops and friction factors within pipes. Crowe et al. [16] discuss flow in conduits and provide equations for head loss, friction factors, and dimensionless head loss coefficients for transitions and fittings. Using this literature all of the piping within the cooling system can be modeled in terms of pressure loss and flow.

The piping and fitting component equations and parameters utilize dimensionless head loss coefficients where the friction factor, dimensionless head loss coefficient, and head loss, respectively, are [16]:

$$f = \frac{0.25}{\left[log_{10}\left(\frac{k_s}{3.7D} + \frac{5.74}{Re^{0.9}}\right)\right]^2} \tag{17}$$

$$K = f\frac{L}{D} \tag{18}$$

$$H_f = K\frac{v_1^2}{2g} \tag{19}$$

In the previous equations, f is the friction factor, k_s is the roughness factor, K is the dimensionless head loss coefficient, L is the length of the pipe, D is the diameter of the pipe, H_f is the head loss, v is the velocity, and g is gravity. The pressure change in the conduit is related to head loss through the modified Bernoulli's equation:

$$p_1 + \rho g z_1 = p_2 + \rho g z_2 + \rho g H_f \tag{20}$$

Where p is pressure, ρ is density, g is gravity, z is the height, and H_f is the head loss computed using Equation (19). The coolant flow rate and pump head are governed by the rotational speed of the cooling water pump. The pump affinity laws, as described by McQuiston et al. [17], can be used to determine the coolant flow rate and the pump head based upon the pump rotational speed. The pump affinity laws for the coolant flow rate and pump head, respectively, are:

$$\dot{V}_n = \dot{V}_o\left(\frac{RPM_n}{RPM_o}\right) \tag{21}$$

$$H_n = H_o\left(\frac{RPM_n}{RPM_o}\right)^2 \tag{22}$$

In Equations (21) and (22), $\dot{V}$ is the volumetric flow rate, RPM is the pump speed, and H is the developed pump head. The subscript n refers to the new value and the subscript o refers to the old value of pump speed, coolant flow rate, or pump head.

2.6 Daily Ambient Temperature Model

The amount of energy transferred as heat from the fin-fan heat exchanger to the environs is a function of the ambient temperature. The daily ambient temperature can be modeled using the ASHRAE outdoor temperature model [17]. The outdoor temperature is assumed to vary in a sinusoidal fashion between the maximum and minimum daily temperatures. The ASHRAE outdoor temperature model can be used to calculate the temperature on an hourly basis. The ASHRAE model is written as:

$$T_{hourly} = T_{max} - DR(X) \tag{23}$$

As shown in Equation (23), the hourly temperature, T_{hourly}, is a function of the maximum temperature, T_{max}, minus the daily range *DR* multiplied by the defined hourly weighting factor of the daily range (*X*).

2.7 OEM Operating Guidelines

During Task 1, OEM operating guides for Cooper and Clark engines were collected in order to further understand the cooling systems. The following information represents the key points taken from the OEM operating guides, provided by various parties involved in the PCRI funded project:

- Nominal coolant inlet temperature into the engine is approximately 160ºF.
- The coolant pump speed is a function of the engine speed. Thus, the engine speed controls the engine coolant inlet pressure and mass flow rate.
- The thermostatic control valve in the cooling system controls the engine coolant inlet temperature and, for the auxiliary cooling side of system 2, the aftercooler coolant inlet temperature.
- A small temperature rise, nominally 10^{0}F across engine, results in a more even water temperature throughout the engine jackets and reduces the possibility of boiling.

The OEM operating guides also provide information concerning various parameters utilized in the cooling system model. These parameters include:

- Approximate engine heat transfer rates to the coolant
- Pressure differentials of cooling equipment
- Pump head and flow rate at full load.

2.8 Literature Review Conclusions

The thermodynamic, heat transfer, and fluid dynamic principles that govern the cooling water system can be manipulated to develop an encompassing cooling system model. From the literature review, the following conclusions can be drawn:

- Controlled nucleate boiling results in the maximum heat transfer from the engine to the cooling water. This could lead to lower coolant pressures and metal temperatures at lower coolant flow rates. OEM operating guidelines state that the coolant flow rate is a function of engine speed and, thus, cannot be varied.

- Dimensionless Nusselt number formations and thermal resistances can be used to model the heat transfer from the in-cylinder combusting gases to the cooling water system.
- The in-cylinder heat transfer coefficient can be calculated using correlations developed by Annand or Woschni.
- All fluid dynamics within the cooling system can be modeled using the modified Bernoulli's equation and other fluid dynamic principles discussed in Section 2.5.

The research team developed the cooling system model which utilizes knowledge obtained during the literature review. The points from the literature review used in the model and further discussed in this thesis are:

- The in-cylinder heat transfer from the combusting gases to the cooling water was modeled using thermal resistances.
- Woschni's equation was implemented into T-RECS to determine the in-cylinder heat transfer coefficient.
- The fluid dynamics of the cooling water system were modeled using the modified Bernoulli's equation as well as other fluid dynamic principles discussed in Section 2.5.
- The heat exchangers were modeled using Equations (6)-(8).
- The pump head and coolant flow rate was determined using the pump affinity laws.
- The daily ambient temperature was modeled using a derived form of the ASHRAE model discussed in Section 2.6.
- The complete cooling water system modeling equations were discretized and solved using the Gauss-Seidel method.

Chapter 3 - Mathematical Model

This section focuses on the heat transfer, thermodynamic, and the fluid dynamic models within individual system components. The first component discussed is the engine and the associated heat transfer.

3.1 In-Cylinder to Coolant Heat Transfer Model

Figure 3.1 shows a graphical representation of a piston cylinder setup and the associated heat transfer mechanisms. As discussed in Section 2.3, the heat transfer from the combustion area to the coolant flowing around the cylinder can be modeled using thermal resistances. Figure 3.2 shows a graphical representation of the thermal resistances.

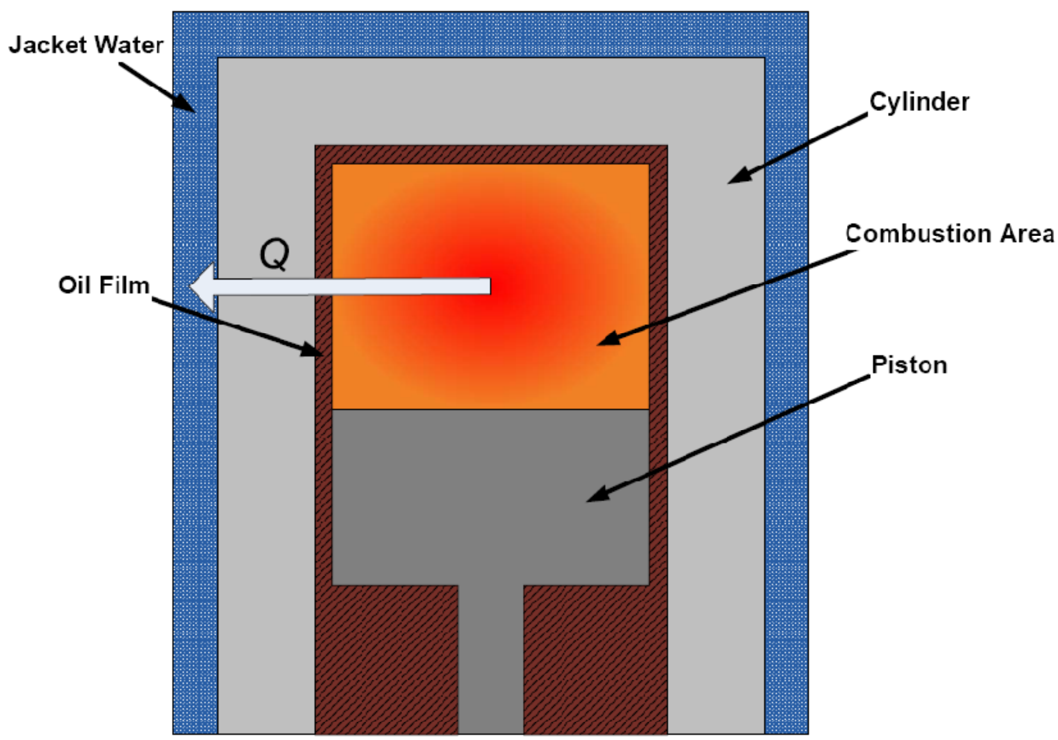

Figure 3.1 – Model of Piston Cylinder Setup

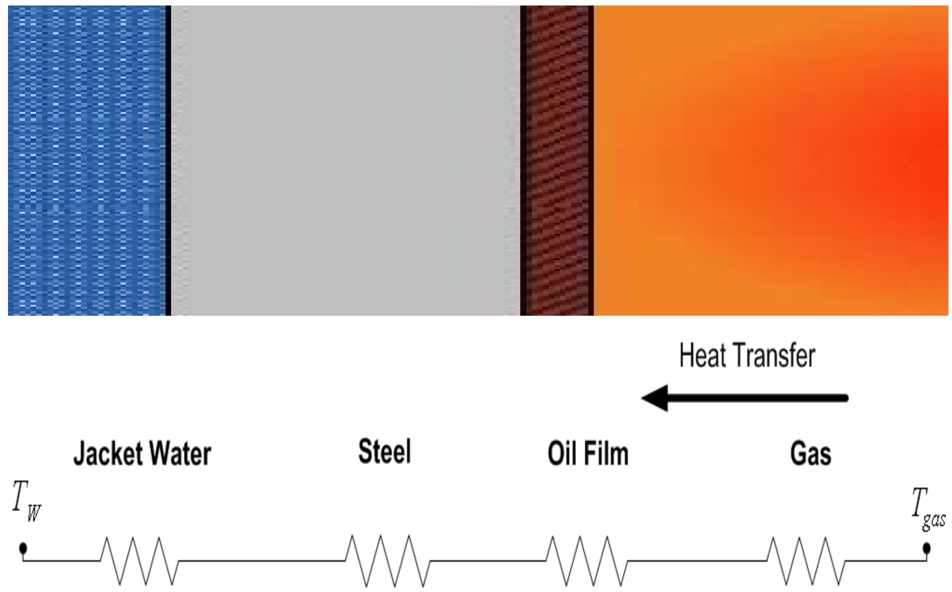

Figure 3.2 – Engine Thermal Resistance Model

Equations (11)-(16), discussed in Section 2.3, were used to determine the heat flux from the combusting gases to the jacket water. The thermal resistances of the oil film, cylinder wall, and jacket water are approximated using known, acceptable ranges for the temperatures, convective heat transfer coefficients, and thermal conductivities. The thickness of the cylinder wall, x, was taken from engine drawings provided by Cameron. These values were used as tuning factors to match the heat transfer rate from the engine to the cooling water described within the OEM operating guides. A fouling factor was also added as another thermal resistivity. The fouling factor represents the scale build-up on the jacket water side of the cylinder walls over time and affects the heat transfer rate and outlet temperature of the jacket water.

The convective heat transfer coefficient of the in-cylinder gases depends upon the period of the engine cycle (i.e. compression, combustion, expansion, gas exchange) and is determined by Woschni's equation [12] as discussed in Section 2.3.

Woschni's equation was implemented into the T-RECS program described in Section 2.4. T-RECS is a FORTRAN based program that, for this thesis, was used to calculate the required in-cylinder pressures and temperatures utilized within Woschni's equation for the given period.

A FORTRAN subroutine was implemented into T-RECS to calculate the heat flux to the engine jacket water as a function of engine crank angle. The cycle-averaged heat flux is then calculated by summing the heat fluxes calculated for each engine crank angle step and dividing by the total number of crank angle steps taken in the cycle. The engine jacket water was assumed to enter the engine at 160ºF throughout the entire cycle. This assumption was based upon the OEM operating guidelines collected during Phase 1 of the PCRI funded project. Also, the radiative heat transfer was assumed to be very small compared to convective heat transfer and thus neglected. The average heat flux, $\ddot{q}_{avg}$, is calculated by summing the heat flux , $\ddot{q}$, and dividing by the total number of crank angle steps, *Crank*, taken through the cycle:

$$\ddot{q}_{avg} = \frac{\sum_{i=0}^{360} \ddot{q}_i}{Crank(360) - Crank(0)} \tag{24}$$

The average rate of heat transfer to the jacket water is calculated based upon the average heat flux, $\ddot{q}_{avg}$, and the surface area of the cylinder, A_{cyl}, as:

$$\dot{q}_{avg} = \ddot{q}_{avg} A_{cyl} \tag{25}$$

3.2 Heat Exchangers Model

The heat exchangers within system 1 include the engine oil cooler and the fin-fan unit while the heat exchangers in system 2 include the engine oil cooler, the aftercooler, and the fin-fan units. A graphical representation of the heat transfer within the heat exchangers is shown in Figure 3.3.

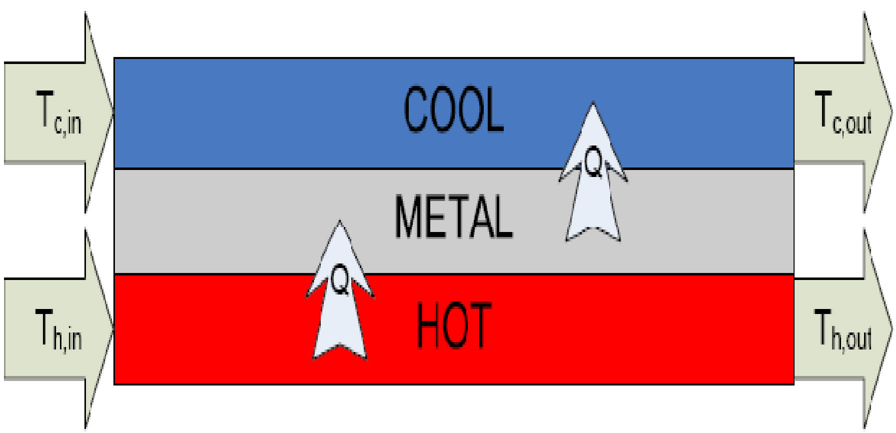

Figure 3.3 – Heat Exchanger Model

As shown in Figure 3.3, the energy is transferred from the entering hot fluid to the intermediate metal and then to the cooling fluid. The cooling water takes on different roles within the fin-fan unit, engine oil cooler, and the aftercooler. In the fin-fan unit, the cooling water acts as the hot fluid and the energy is transferred to the outdoor air. In the engine oil cooler, the hot oil exiting the engine transfers energy to the cooling water. In the aftercooler, the hot air leaving the turbocharger transfers energy to the cooling water. The general equations describing the heat transfer within the heat exchangers are discussed in Section 2.2.

Due to the lack of available information pertaining to the heat exchangers, values were assumed for the effective heat transfer areas and the convective heat transfer coefficients. Values for the ambient air flow rate through the fin-fan unit and oil flow rate through the oil cooler were also assumed and held constant. Table 3.1 shows the values assumed for the above mentioned parameters. The parameters mentioned in this paragraph directly affect the resulting outlet temperatures and heat transfer rates for the heat exchangers.

Table 3.1 – Assumed Heat Exchanger parameters

Fin-Fan	**Coolant-Side**	**Air-Side**
Area (ft^2)	500	1000
Heat Transfer Coefficient (BTU/hr-ft^2-F)	90	40
Air Flow Rate (SCFM)	140000	
Oil Cooler	**Coolant-Side**	**Oil-Side**
Area (ft^2)	50	80
Heat Transfer Coefficient (BTU/hr-ft^2-F)	90	140
Oil Flow Rate (GPM)	300	

3.3 Thermostatic Control Valve Model

The thermostatic control valve (TCV) controls the inlet temperature of the coolant into the engine in system 1 and jacket water side of system 2. In the auxiliary cooling side of system 2, the TCV controls the coolant inlet temperature into the aftercooler. As shown in Figure 3.4, the coolant flowing from the cooling equipment is mixed with coolant re-circulated from the engine outlet. For system 2's auxiliary cooling TCV, the coolant flowing from the fin-fan unit is mixed with re-circulating coolant from the engine oil cooler.

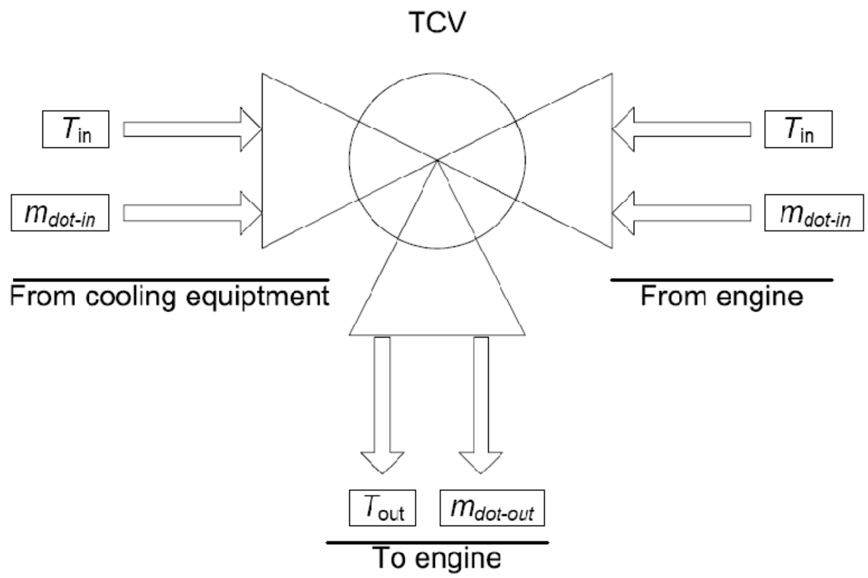

Figure 3.4 – TCV Illustration

The TCV is assumed to be a steady state, adiabatic mixing process with negligible changes in kinetic and potential energy, and constant specific heats. Applying the conditions mentioned above to the first law of thermodynamics, Equation (1) is re-written as:

$$\dot{m}_{sys}T_{sys} + \dot{m}_{rec}T_{rec} = \dot{m}_{eng,in}T_{eng,in} \qquad (1a)$$

Where $\dot{m}$ is the mass flow rate and T is the temperature. Equation (1a) represents the governing equation used to model the thermodynamic aspects of the TCV within the complete cooling system discussed later in Section 4.4. Aspects concerning the fluid dynamics of the TCV are discussed in the following section.

3.4 Coolant Piping System Model

This section focuses on the fluid dynamic approach used to model the cooling water piping system. Figure 3.5 shows a schematic of system 1 with numbers representing points used to model the fluid dynamics of the system. The piping system model for system 2 was also developed in the same fashion, but is not shown.

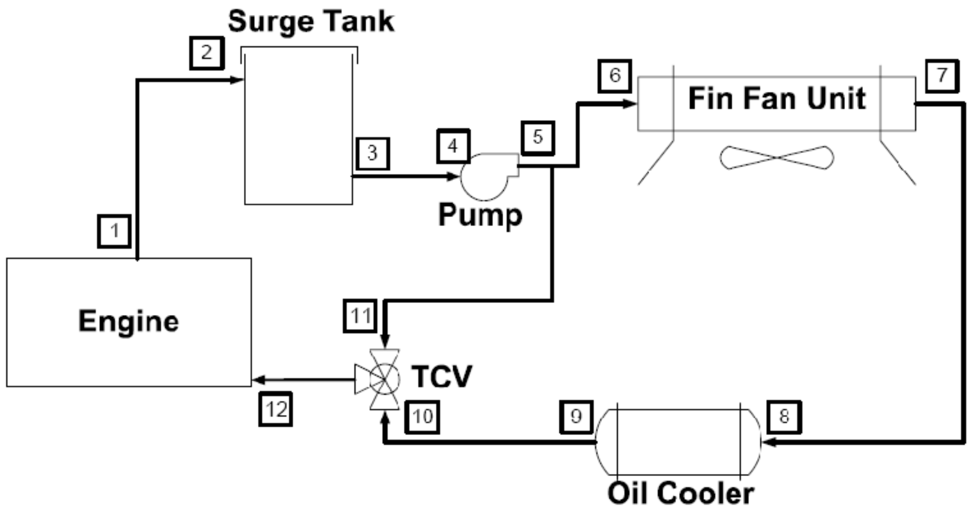

Figure 3.5 – Schematic of system 1

3.4.1 Coolant Piping, Fittings, Valves, and Surge Tank Model

The resulting pressures at the various points identified in Figure 3.5 are determined by utilizing the modified Bernoulli's equation, Equation (20), discussed in Section 2.5.

The head losses experienced within the piping system are determined by utilizing the dimensionless friction factors. Table 3.1 shows the dimensionless friction factors used to develop the model, for 90 degree bends, 45 degree bends, valves, and the TCV.

Table 3.2 – Dimensionless Friction Factors [18]

K_{90}	K_{45}	K_{valve}	K_{TCV}
0.2	0.14	6.0	8.0

Along with the fitting friction factors, the friction factor due to the pipe roughness must be taken into account. The piping friction factor is determined by using Equation (18). The friction factor, f, is assumed to be 0.02, a suitable value for steel piping, throughout the entire piping system.

With knowledge of the pipe sections, the total friction factor is calculated along with the resulting frictional head loss of the piping section:

$$K_{total} = K_{90}N_{90} + K_{45}N_{45} + K_{valve}N_{valve} + K_{pipe} \tag{26}$$

$$H_f = K_{total}\frac{\left(\frac{\dot{m}}{\rho A}\right)^2}{2g} = K_{total}\frac{(v)^2}{2g} \tag{27}$$

In Equations (26) and (27), K is the dimensionless friction factor, N is the number fittings in a section of pipe, H_f, is the head loss, $\dot{m}$ is the mass flow rate, ρ is the density, A is the cross sectional area of the pipe, g is gravity, and v is the velocity in the pipe.

The surge tank provides the system with room to expand as well as to establish a minimum suction pressure for the coolant pump. The outlet pressure of the surge tank, $p_{surge,out}$ depends upon the ambient pressure, p_{amb}, and the height of the water within the surge tank, z_{surge}. The outlet pressure is calculated by:

$$p_{surge,out} = p_{amb} + \rho g z_{surge} \tag{28}$$

3.4.2 Coolant Pump and Cooling Equipment Model

As stated in the literature review, the pump speed is driven by the speed of the engine. Thus, as the engine speed varies, the pump speed, RPM_p, must vary as a function of the engine speed, RPM_{eng}. By assuming a linear correlation between the engine and pump speeds, with the pump speed being zero when the engine speed is zero, the pump speed is calculated by:

$$RPM_p = \left(\frac{RPM_{p,known}}{RPM_{eng,known}}\right)RPM_{eng} \tag{29}$$

It should be noted that the engine and corresponding pump speed must be known (represented in Equation (29) by the subscript *known*) at one condition to develop the relationship factor. Once the pump speed is determined, the pump affinity laws are used to calculate the pump head and coolant flow rate. The pump affinity laws are discussed in Section 2.5.

The cooling equipment includes the engine, fin-fan unit, and the oil cooler for system 1. The same equipment mentioned with the addition of the aftercooler makes up the cooling equipment for system 2. The OEM operating guidelines provide a maximum value for the pressure losses across the cooling equipment. In order to model the pressure differential across the cooling equipment, Δp_{ce}, as a function of coolant mass flow rate, the following equation was derived from Equation 27:

$$\Delta p_{ce} = K_{ce} \frac{\left(\frac{\dot{m}}{\rho A}\right)^2}{2} \rho = \beta \dot{m}^2 \tag{30}$$

The resulting pressure loss coefficient β is no longer dimensionless like the friction factor K, but does represent the pressure loss through a given component as a function of coolant mass flow rate for a given cooling system setup.

Chapter 4 - Model Development

This section focuses on the development of the discretized system of equations and the iterative method used to solve the system. Also, this section discusses the development of the daily ambient temperature model.

4.1 Model Overview

Utilizing the equations discussed in the previous sections, a set of 23 equations with 23 unknowns for system 1 and 43 equations and 43 unknowns for system 2 was developed that describe the heat transfer, fluid dynamics, and thermodynamics involved in the system. This set of equations is used within the model to solve for:

- Pressures at various points within the system
- Temperatures entering and exiting the cooling equipment
- Mass flow rates within the system
- Heat transferred from the fin fan unit to the ambient surroundings

Figure 4.1 shows the schematic of system 1 with numbers representing the points throughout the system used to model the fluid dynamics of the system. Figure 4.1 is used to graphically illustrate the developed system of equations for system 1 shown in Table 4.1. System 2 is shown in Figure 4.2 and the corresponding system of equations for the jacket water and auxiliary cooling system are shown in Tables 4.2 and 4.3, respectively.

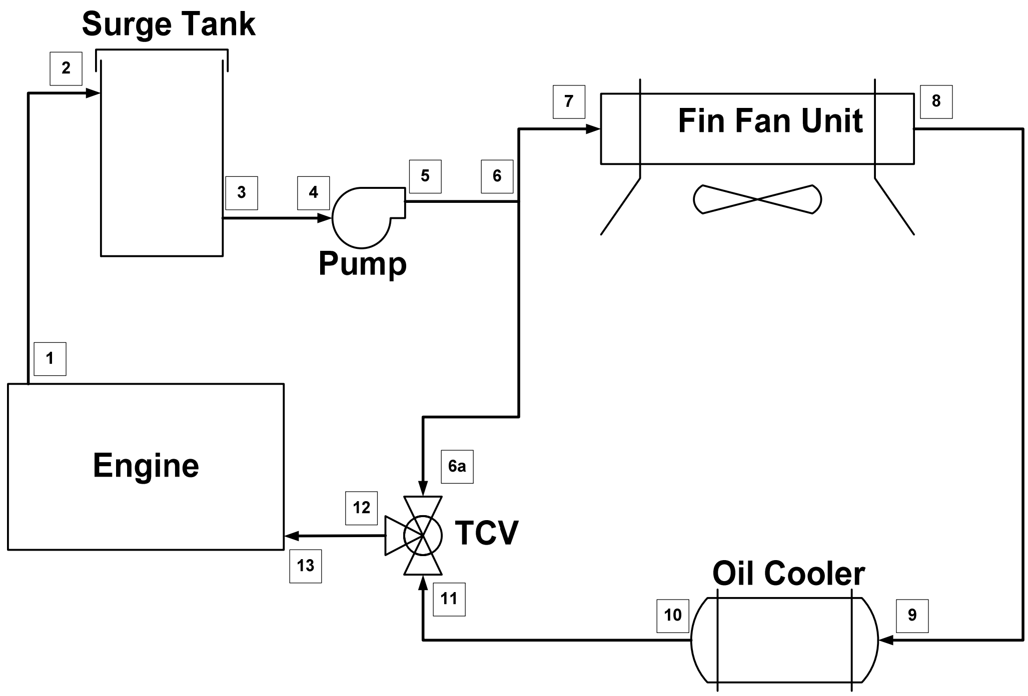

Figure 4.1 – Diagram of System 1 (Numbered)

Table 4.1 – Equations for System 1

$p_2 = p_1 - \rho g \left(K_{12} \frac{\left(\frac{\dot{m}}{\rho A_{12}}\right)^2}{2g} - z_1 + z_2 \right)$	(31)
$p_3 = p_{amb} + \rho g z_{surge}$	(32)
$p_4 = p_3 - \rho g \left(K_{34} \frac{\left(\frac{\dot{m}}{\rho A_{34}}\right)^2}{2g} - z_3 + z_4 \right)$	(33)
$p_5 = p_4 + \rho g H_{pump}$	(34)
$p_6 = p_5 - \rho g \left(K_{56} \frac{\left(\frac{\dot{m}}{\rho A_{56}}\right)^2}{2g} - z_5 + z_6 \right)$	(35)

$p_7 = p_6 - \rho g \left((K_{67} + K_T) \frac{\left(\frac{\dot{m}_{sys}}{\rho A_{67}}\right)^2}{2g} - z_6 + z_7 \right)$	(36)
$p_{6a} = p_6 - \rho g \left((K_{66a} + K_T) \frac{\left(\frac{\dot{m}_{rec}}{\rho A_{66a}}\right)^2}{2g} - z_6 + z_{6a} \right)$	(37)
$p_8 = p_7 - \beta_{finfan} \dot{m}^2$	(38)
$p_9 = p_8 - \rho g \left(K_{89} \frac{\left(\frac{\dot{m}_{sys}}{\rho A_{89}}\right)^2}{2g} - z_8 + z_9 \right)$	(39)
$p_{10} = p_9 - \beta_{OC} \dot{m}^2$	(40)
$p_{11} = p_{10} - \rho g \left(K_{1011} \frac{\left(\frac{\dot{m}_{sys}}{\rho A_{1011}}\right)^2}{2g} - z_{10} + z_{11} \right)$	(41)
$p_{12} = p_{11} - \rho g \left(K_{TCV} \frac{\left(\frac{\dot{m}}{\rho A}\right)^2}{2g} \right)$	(42)
$p_{13} = p_{12} - \rho g \left(K_{1213} \frac{\left(\frac{\dot{m}}{\rho A_{1213}}\right)^2}{2g} - z_{12} + z_{13} \right)$	(43)
$p_1 = p_{13} - \beta_{eng} \dot{m}^2$	(44)
$\dot{m}_{sys} = \frac{\dot{m}(T_1 - T_{13})}{T_1 - T_{10}}$	(45)
$\dot{m}_{rec} T_1 = \dot{m} T_{13} - \dot{m}_{sys} T_{10}$	(46)

$T_8\left(\frac{M_w c_w}{\Delta t} + \dot{m}_{sys} c_w + h_w A_w\right) = \dot{m}_{sys} c_w T_1 + h_w A_w T_m + \frac{M_w c_w T_8^o}{\Delta t}$	(47)
$T_m\left(h_w A_w + h_a A_a + \frac{M_m c_m T_m}{\Delta t}\right) = T_8 h_w A_w + h_a A_a T_a + \frac{M_m c_m T_m^o}{\Delta t}$	(48)
$T_a\left(\frac{M_a c_a}{\Delta t} + \dot{m}_a c_a + h_a A_a\right) = \dot{m}_a c_a T_{a,in} + h_a A_a T_m + \frac{M_a c_a T_a^o}{\Delta t}$	(49)
$T_{10}\left(\frac{M_w c_w}{\Delta t} + \dot{m}_{sys} c_w + h_w A_w\right) = \dot{m}_{sys} c_w T_8 + h_w A_w T_m + \frac{M_w c_w T_{10}^o}{\Delta t}$	(50)
$T_m\left(h_w A_w + h_o A_o + \frac{M_m c_m T_m}{\Delta t}\right) = T_w h_w A_w + h_o A_o T_o + \frac{M_m c_m T_m^o}{\Delta t}$	(51)
$T_o\left(\frac{M_o c_o}{\Delta t} + \dot{m}_o c_o + h_o A_o\right) = \dot{m}_o c_o T_{o,in} + h_o A_o T_m + \frac{M_o c_o T_o^o}{\Delta t}$	(52)
$T_1 = T_{13} + \frac{\dot{Q}_{eng}}{\dot{m} c_w}$	(53)

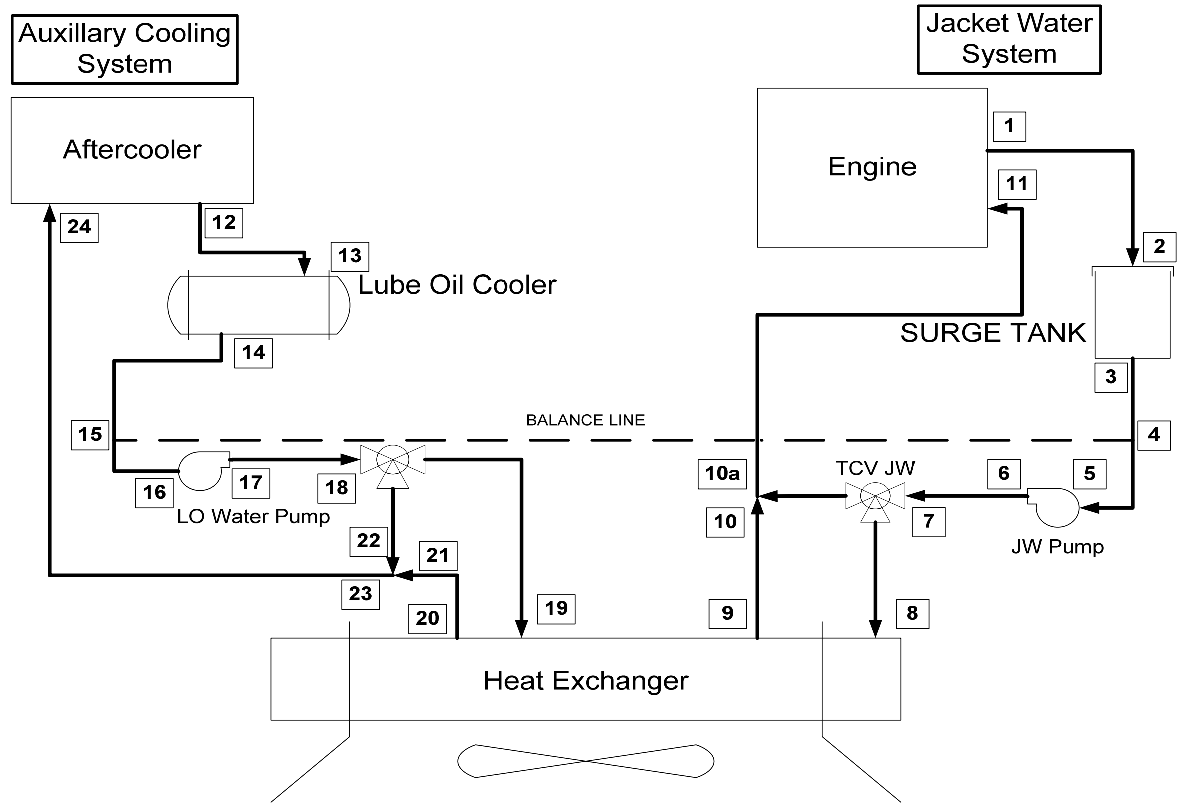

Figure 4.2 – Diagram of System 2 (Numbered)

Table 4.2 – System 2 Equations ~ Jacket Water Side

$$p_2 = p_1 - \rho g\left(K_{12}\frac{\left(\frac{\dot{m}}{\rho A_{12}}\right)^2}{2g} - z_1 + z_2\right)$$	(54)
$$p_3 = p_{amb} + \rho g z_{surge}$$	(55)
$$p_4 = p_3 - \rho g\left(K_{34}\frac{\left(\frac{\dot{m}}{\rho A_{34}}\right)^2}{2g} - z_3 + z_4\right)$$	(56)
$$p_5 = p_4 - \rho g\left(K_{45}\frac{\left(\frac{\dot{m}}{\rho A_{45}}\right)^2}{2g} - z_4 + z_5\right)$$	(57)
$$p_6 = p_5 + \rho g H_{pump}$$	(58)

$p_7 = p_6 - \rho g\left(K_{67}\frac{\left(\frac{\dot{m}_{sys}}{\rho A_{67}}\right)^2}{2g} - z_6 + z_7\right)$	(59)
$p_8 = p_7 - \rho g\left((K_{78} + K_{TCV})\frac{\left(\frac{\dot{m}_{sys}}{\rho A_{78}}\right)^2}{2g} - z_7 + z_8\right)$	(60)
$p_{7a} = p_7 - \rho g\left((K_{77a} + K_{TCV})\frac{\left(\frac{\dot{m}_{rec}}{\rho A_{77a}}\right)^2}{2g} - z_7 + z_{7a}\right)$	(61)
$p_9 = p_8 - \beta_{finfan}\dot{m}^2$	(62)
$p_{10} = p_9 - \rho g\left(K_{910}\frac{\left(\frac{\dot{m}_{sys}}{\rho A_{910}}\right)^2}{2g} - z_9 + z_{10}\right)$	(63)
$p_{10a} = p_{10} - \rho g\left(K_T\frac{\left(\frac{\dot{m}_{sys}}{\rho A_{10}}\right)^2}{2g}\right)$	(64)
$p_{11} = p_{10a} - \rho g\left(K_{10a11}\frac{\left(\frac{\dot{m}}{\rho A_{10a11}}\right)^2}{2g} - z_{10a} + z_{11}\right)$	(65)
$p_1 = p_{11} - \beta_{eng}\dot{m}^2$	(66)
$\dot{m}_{sys} = \frac{\dot{m}(T_1 - T_{11})}{T_1 - T_9}$	(67)
$\dot{m}_{rec}T_1 = \dot{m}T_{11} - \dot{m}_{sys}T_9$	(68)
$T_9\left(\frac{M_w c_w}{\Delta t} + \dot{m}_{sys}c_w + h_w A_w\right) = \dot{m}_{sys}c_w T_1 + h_w A_w T_m + \frac{M_w c_w T_9^o}{\Delta t}$	(69)

$T_m\left(h_wA_w + h_aA_a + \frac{M_mc_mT_m}{\Delta t}\right) = T_9h_wA_w + h_aA_aT_a + \frac{M_mc_mT_m^o}{\Delta t}$	(70)
$T_a\left(\frac{M_ac_a}{\Delta t} + \dot{m}_ac_a + h_aA_a\right) = \dot{m}_ac_aT_{a,in} + h_aA_aT_m + \frac{M_ac_aT_a^o}{\Delta t}$	(71)
$T_1 = T_{11} + \frac{\dot{Q}_{eng}}{\dot{m}c_w}$	(72)

Table 4.3 – System 2 Equations ~ Auxiliary Cooling Side

$p_{13} = p_{12} - \rho g\left(K_{1213}\frac{\left(\frac{\dot{m}}{\rho A_{1213}}\right)^2}{2g} - z_{12} + z_{13}\right)$	(73)
$p_{14} = p_{13} - \beta_{OC}\dot{m}^2$	(74)
$p_{15} = p_{14} - \rho g\left(K_{1415}\frac{\left(\frac{\dot{m}}{\rho A_{1415}}\right)^2}{2g} - z_{14} + z_{15}\right)$	(75)
$p_{15a} = p_4$	(76)
$p_{16} = p_{15a} - \rho g\left(K_{15a16}\frac{\left(\frac{\dot{m}}{\rho A_{15a16}}\right)^2}{2g} - z_{15a} + z_{16}\right)$	(77)
$p_{17} = p_{16} + \rho g H_{pump}$	(78)
$p_{18} = p_{17} - \rho g\left(K_{1718}\frac{\left(\frac{\dot{m}}{\rho A_{1718}}\right)^2}{2g} - z_{17} + z_{18}\right)$	(79)

$$p_{19} = p_{18} - \rho g \left((K_{1819} + K_{TCV}) \frac{\left(\frac{\dot{m}_{sys}}{\rho A_{1819}}\right)^2}{2g} - z_{18} + z_{19} \right)$$	(80)
$$p_{22} = p_{18} - \rho g \left((K_{1822} + K_{TCV}) \frac{\left(\frac{\dot{m}_{rec}}{\rho A_{1822}}\right)^2}{2g} - z_{18} + z_{22} \right)$$	(81)
$$p_{20} = p_{19} - \beta_{finfan} \dot{m}^2$$	(82)
$$p_{21} = p_{20} - \rho g \left(K_{2021} \frac{\left(\frac{\dot{m}_{sys}}{\rho A_{2021}}\right)^2}{2g} - z_{20} + z_{21} \right)$$	(83)
$$p_{23} = p_{21} - \rho g \left((K_{2123} + K_{T}) \frac{\left(\frac{\dot{m}}{\rho A_{2123}}\right)^2}{2g} - z_{21} + z_{23} \right)$$	(84)
$$p_{12} = p_{23} - \beta_{AC} \dot{m}^2$$	(85)
$$\dot{m}_{sys} = \frac{\dot{m}(T_{14} - T_{24})}{T_{14} - T_{20}}$$	(86)
$$\dot{m}_{rec} T_{14} = \dot{m} T_{23} - \dot{m}_{sys} T_{20}$$	(87)
$$T_{20} \left(\frac{M_w c_w}{\Delta t} + \dot{m}_{sys} c_w + h_w A_w \right) = \dot{m}_{sys} c_w T_{14} + h_w A_w T_m + \frac{M_w c_w T_{20}^o}{\Delta t}$$	(88)
$$T_m \left(h_w A_w + h_a A_a + \frac{M_m c_m T_m}{\Delta t} \right) = T_{20} h_w A_w + h_a A_a T_a + \frac{M_m c_m T_m^o}{\Delta t}$$	(89)
$$T_a \left(\frac{M_a c_a}{\Delta t} + \dot{m}_a c_a + h_a A_a \right) = \dot{m}_a c_a T_{a,in} + h_a A_a T_m + \frac{M_a c_a T_a^o}{\Delta t}$$	(90)
$$T_{14} \left(\frac{M_w c_w}{\Delta t} + \dot{m} c_w + h_w A_w \right) = \dot{m} c_w T_{13} + h_w A_w T_m + \frac{M_w c_w T_{14}^o}{\Delta t}$$	(91)

$T_m\left(h_wA_w + h_oA_o + \frac{M_mc_mT_m}{\Delta t}\right) = T_{14}h_wA_w + h_oA_oT_o + \frac{M_mc_mT_m^o}{\Delta t}$	(92)
$T_o\left(\frac{M_oc_o}{\Delta t} + \dot{m}_oc_o + h_oA_o\right) = \dot{m}_oc_oT_{o,in} + h_oA_oT_m + \frac{M_oc_oT_o^o}{\Delta t}$	(93)
$T_{12}\left(\frac{M_wc_w}{\Delta t} + \dot{m}c_w + h_wA_w\right) = \dot{m}c_wT_{23} + h_wA_wT_m + \frac{M_wc_wT_{12}^o}{\Delta t}$	(94)
$T_m\left(h_wA_w + h_oA_o + \frac{M_mc_mT_m}{\Delta t}\right) = T_{12}h_wA_w + h_{exh}A_{exh}T_{exh} + \frac{M_mc_mT_m^o}{\Delta t}$	(95)
$T_{exh}\left(\frac{M_{exh}c_{exh}}{\Delta t} + \dot{m}_{exh}c_{exh} + h_{exh}A_{exh}\right) = \dot{m}_{exh}c_{exh}T_{exh,in} + h_{exh}A_{exh}T_m + \frac{M_{exh}c_{exh}T_{exh}^o}{\Delta t}$	(96)

4.2 Development of the Iterative solution method

The two systems of equations described in section 4.1 were discretized using methods discussed by Patankar [8] (refer to Section 2.2.)

The linearized set of equations is then solved using the Gauss-Siedel iteration method [8]. Figure 4.3 depicts the iterative system of equations solver used within the cooling system model. As shown in Figure 4.3, the iterative process is broken down into the following steps:

1. The unknowns are set to initial guess values.
2. For the first iteration only, the old unknown values are set to the initial guess values.
3. The coefficients of the unknowns and the constants in the equations are calculated.
4. New values for the unknowns are calculated based upon the old unknown values.
5. The iteration error is calculated using the following steps:
    a. Calculate the absolute value of the difference between the newly calculated value and the previously calculated value for the unknown.
    b. Divide by the newly calculated value for the unknown.
    c. Repeat for each unknown.
    d. Add individual errors to determine total error in iteration.
6. Error Handling:

a. If the error in the iteration is greater than the maximum error allowed, the iterative process repeats itself and sets the old unknown values equal to the newly calculated unknown values.

b. If the error in the iteration is less than the maximum error allowed, the calculated unknown values are a solution to the system of equations.

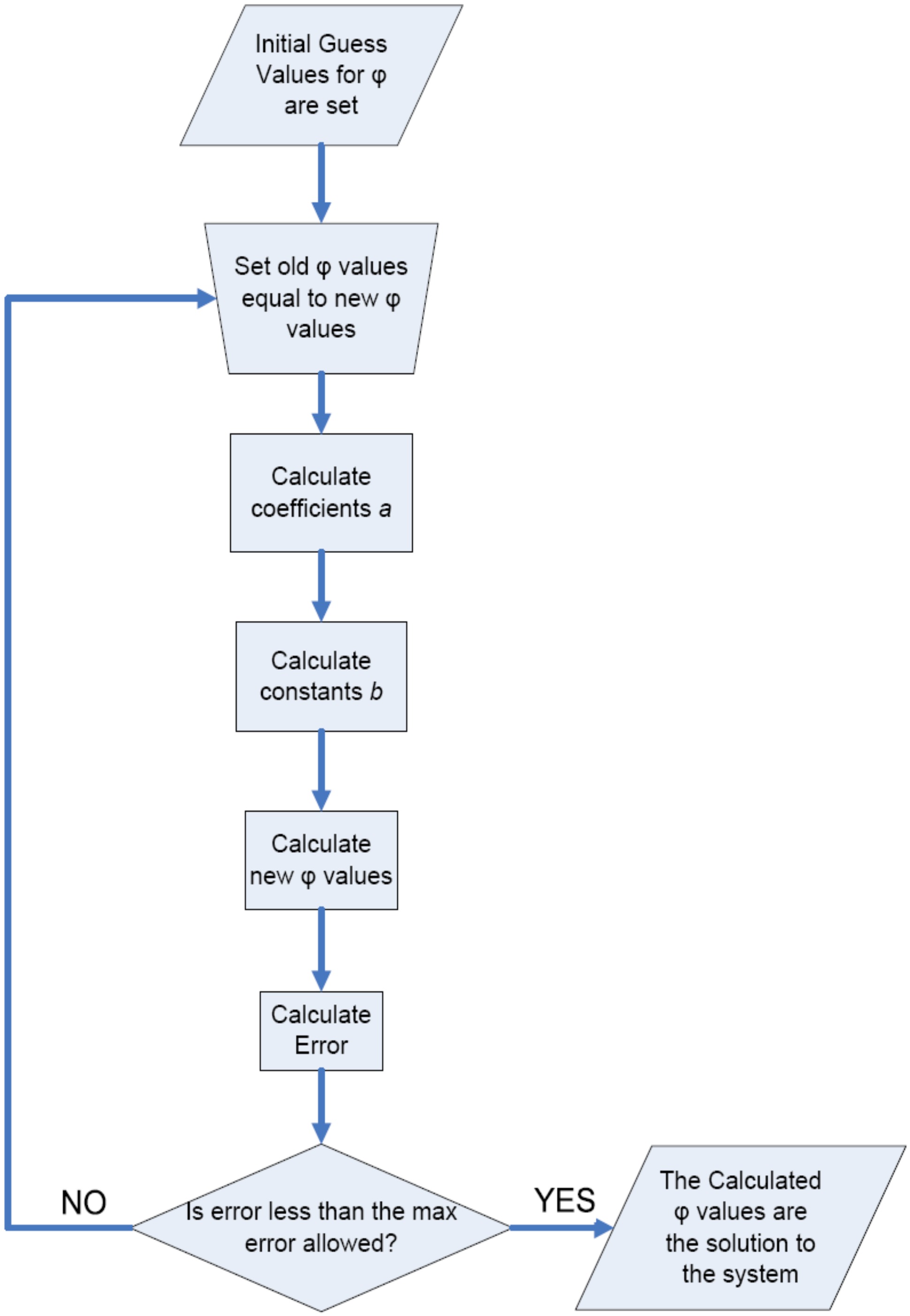

Figure 4.3 – Flow Chart Representing the Iterative Process

4.3 Ambient Temperature Model

The ASHRAE model, Equation 23 discussed in Section 2.6, was modified to fit a sine function and varies directly with respect to time instead of a daily percentage. The developed temperature model in Kelvins is [19]:

$$T = 302 + 8\sin\left(0.00436t - 2.3\right) \tag{97}$$

Equation (97) was developed by assuming the maximum daily temperature to be 100ºF (310 K), the minimum temperature to be 70ºF (294 K), and the time of day, t, is in minutes. The cooling system model allows the user to specify the daily temperature range and then develops the temperature model based upon user specifications. Utilizing this model in the cooling system enables the user to view how the cooling system responds to changes in ambient temperature throughout the day.

4.4 Cooling System Computer Model

The previously derived equations were solved utilizing a FORTRAN code with the T-RECS program. Figure 4.4 shows a flow diagram of the cooling system computer model. The cooling system model is broken down into the following steps:

1. The user provides the necessary inputs.
2. The total friction factors and the cooling equipment pressure loss factors are calculated using Equations (26) and (30), respectively.
3. The energy added to the cooling system, by the engine, is calculated using Equations (9)-(16) and (24)-(25).
4. The head and flow rate provided by the pump is calculated using Equations (21) and (22), respectively.
5. Solve the system of equations, involving Equations (31)-(53) for system 1, Equations (54)-(96) for system 2, using the Gauss-Seidel Iterative Method shown in Figure 4.3.
6. Print the model calculated results.

The end-user program is Excel-based, but is able to access the FORTRAN code that is embedded within the Excel-based program in the form of a dynamic link library (DLL). The DLL contains all of the modeling performed in FORTRAN, but does not allow the user to access or change the developed modeling equations. In order to use the program, the user must give the program the required inputs, which include:

- Engine geometry and operating characteristics
- Piping information including pipe diameters, fittings, and pipe lengths
- Ambient conditions
- Coolant chemistry
- Oil flow rate and temperature exiting engine

The coolant chemistry input allows the user to specify, in percentages, the actual components that make up the coolant. The components included in the model are water, glycol, and methanol. From the user specified coolant chemistry, the coolant density and specific heat are determined and implemented into the model.

The inputs are passed to the DLL where all calculations are performed. Once the calculations are complete, the results are then passed back to the Excel program where they can be viewed by the user. The outputs of this software include:

- Coolant pressures throughout the cooling system
- Coolant temperatures entering and exiting the cooling equipment
- The rate of heat dissipation to the ambient surroundings
- The rate of heat transfer from the engine.
- The pump head and flow rate
- System and recirculation mass flow rates
- Saturation pressure based upon calculated exit coolant temperature of the engine

The outputs of the cooling system model can then be used to size cooling equipment for system upgrades and determine whether the installed cooling equipment is able to handle the heat loads experienced within the system. For example, if the heat transferred to the coolant, by the engine and the oil cooler, is greater than the maximum amount of energy that can be expelled by the fin fan unit, then the fin fan unit is either not working properly or cannot handle the heat load produced by the system. The saturation pressure at the engine outlet is included in the output because it can tell the operator where the system is operating with respect to the boiling region. For example, when the outlet pressure of the engine is much greater than the saturation pressure, the coolant throughout the engine is all liquid; moreover, if the outlet pressure is close to the saturation pressure the likelihood that boiling occurs within the engine increases which can cause damaging hot spots.

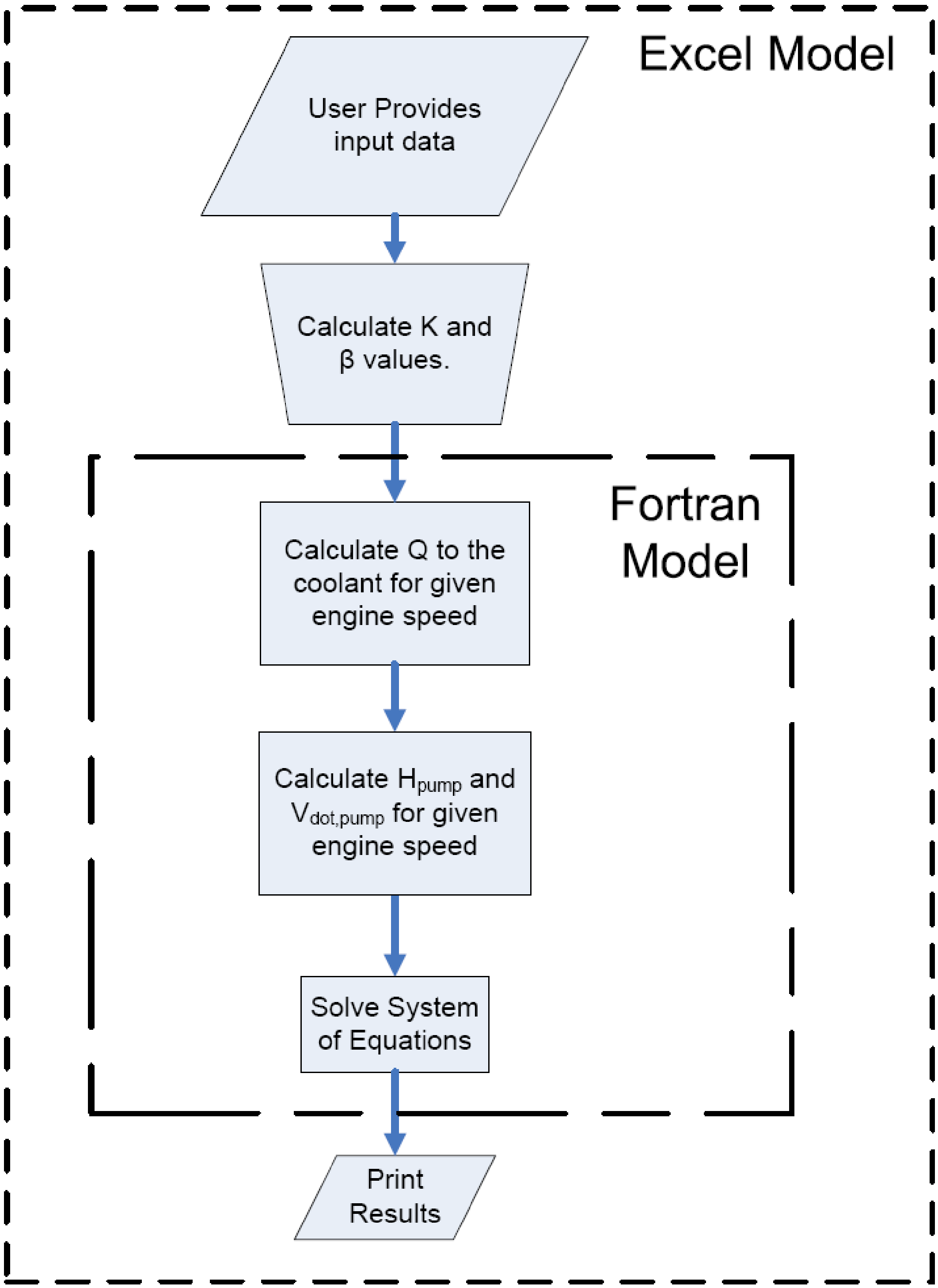

Figure 4.4 – Cooling System Flow Diagram

Chapter 5 - Results and Discussion

This section focuses on the results of a parametric study conducted on the response of the cooling systems to changes in ambient conditions as well as comparing how the systems function at full and part load operating conditions. The engine chosen for this study is the Cooper-Bessemer GMVH 12 cylinder engine. The Cooper-Bessemer GMVH is used in compressor stations along the natural gas pipeline. The engine utilized the natural gas as a fuel and compresses the natural gas to send it down the pipeline. This engine was chosen because all the necessary engine characteristics, equipment pressure differentials, and coolant pump information was readily available from the OEM operating guides. Table 5.1 lists some of the key operating parameters and engine geometry for the Cooper-Bessemer GMVH 12 cylinder engine.

Table 5.1 – GMVH Key Operating Parameter and Geometry

Cooper-Bessemer GMVH 12 Cylinder		
Speed	330	RPM
Brake Horse Power	2700	HP
Torque	42970	lbf-ft
Fuel Flow Rate	326	CFM
Bore	14	in
Stroke	14.7	in
Rod Length	34.375	in

Table 5.2 shows the engine coolant inlet and outlet pressures and the outlet temperature calculated by the model for system 1 as well as from field data [20]. The inlet temperature to the engine, in both the model and field data, is 160ºF. Table 5.2 shows the percent difference between the model calculated parameters and the field data. The data shows that the inlet pressure and outlet temperature calculated with the model are within 5% when compared to the field data. The outlet pressure is within 10% of the field data. Examining the difference between the inlet and outlet pressure in Table 5.2, it is seen that the field data pressure differential is 1 psi greater than the model pressure differential. This increased pressure differential, along with the decreased temperature differential across the engine, could be a sign of fouling within the engine water jackets. This fouling can be accounted for by the model.

Table 5.2 – Results from Model and Field Data

	Model	Field Data	% Difference
Inlet Pressure (psia)	46.05	43.85	4.9
Outlet Pressure (psia)	34.05	30.85	9.9
Outlet Temperature (^{0}F)	170.4	168.2	1.3

Table 5.3 shows the model results and the field data again, but this time a fouling factor of 0.0021 (ft^2- ºF)/BTU was included and the engine pressure differential was increased to match field data. As shown in Table 5.3, the addition of the fouling factor changed the model calculated outlet temperature to within 0.5% of the field data. Also, the increased engine pressure differential lead to the outlet pressure being within 7% of the field data. From these simple 'tuning' techniques, it is easy to see that the model can be fitted to a specific cooling system as long as pressure and temperature measurements are available from points throughout the system.

Table 5.3 – Results from Model (with fouling) and Field Data

	Model	Field Data	% Difference
Inlet Pressure (psia)	46.05	43.85	4.9
Outlet Pressure (psia)	33.05	30.85	6.9
Outlet Temperature (ºF)	168.8	168.2	0.37

5.1 Ambient Conditions and System 1

Figure 5.1 depicts how the heat transfer rate from the fin fan unit is affected by the changes in ambient temperature throughout the day. As stated in Section 4.6, the ambient conditions were assumed to have a peak temperature of 100ºF and a low temperature of 70ºF. Figure 5.1 illustrates that the ambient air temperature governs the amount of heat dissipated to the environs. When the ambient temperature is at its lowest daily value, the maximum amount of energy, 68.3 MBTU/min, is dissipated by the fin fan unit. As the ambient temperature changes a maximum of 30ºF throughout the day, the heat transfer rate from the fin-fan unit decreases by 12%, or decreases to 59 MBTU/min.

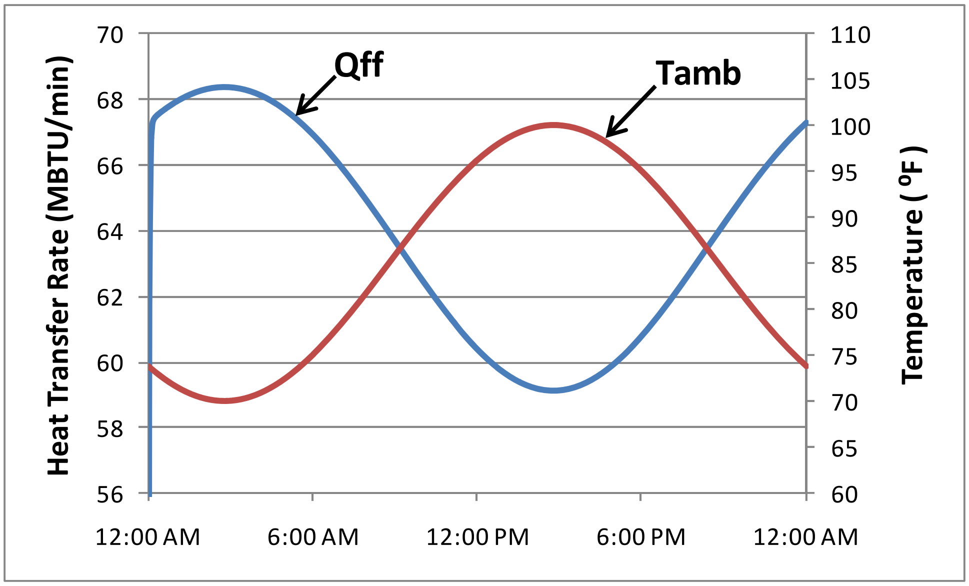

Figure 5.1 – Heat Transfer and Ambient Temperature vs. Time for System 1

As seen in Figure 5.1, the rate of heat transfer from the cooling water to the environs behaves in a sinusoidal manner. To explain this behavior, the layout of system 1 is revisited and shown in Figure 5.2. As discussed in Section 3.3, the thermostatic control valve (TCV) controls the inlet temperature of the engine by mixing the flow rates of the recirculating coolant and the coolant from the fin-fan unit to create a specified engine coolant inlet temperature. Since the coolant mass flow rate through the engine is constant for a constant engine speed and the TCV maintains a constant coolant inlet temperature into the engine, the heat transfer from the engine to the cooling system is constant. Thus, the sine wave behavior must result from the interaction between the fin-fan unit and the oil cooler. Within the model, as discussed in Section 3.2, the flow rate of the ambient air through the fin-fan unit and the oil through the oil cooler were assumed to be constant. Since the air flow rate does not vary, the coolant temperature exiting the fin-fan unit will increase as the ambient temperature increases. This increase in coolant temperature leads to a decreased temperature differential between the oil and coolant entering the oil cooler. Thus, the heat transfer rate from the oil to the coolant will decrease as the coolant temperature increases. Figure 5.3 illustrates the heat transfer rate of the engine and the oil cooler to the coolant during daily ambient temperature changes.

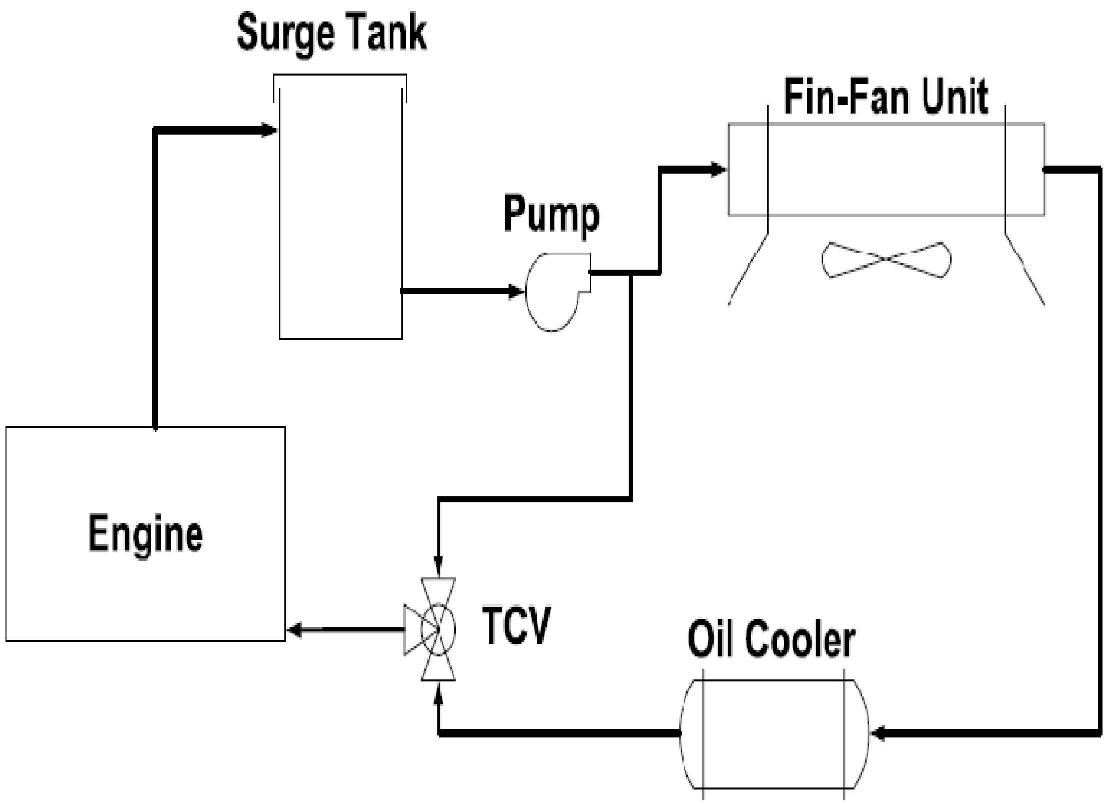

Figure 5.2 – Layout of System 1

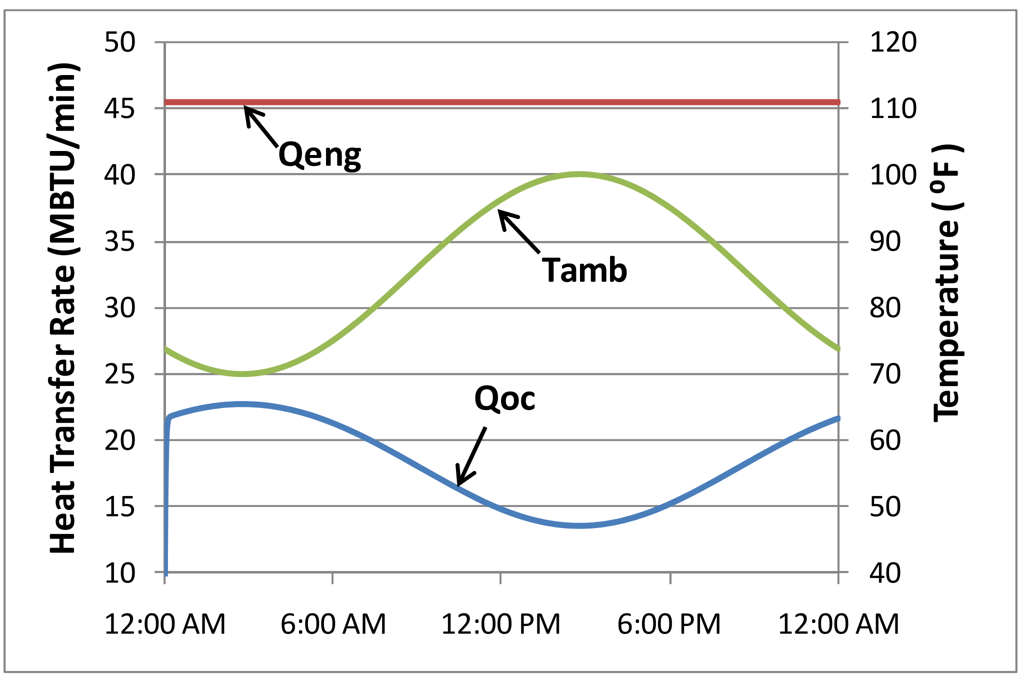

Figure 5.3 – System 1 Heat Transfer Rates for System 1

Figure 5.4 shows the temperature of the oil entering and exiting the oil cooler and the temperature of the coolant entering the oil cooler during daily operation. The oil temperature into the oil cooler is the temperature of the oil exiting the engine and was assumed, based upon collected OEM operating guidelines, to be 160^{0}F. When the ambient temperature is at a minimum of 70^{0}F, the coolant temperature entering the oil cooler is at a minimum of 105^{0}F. At this point, the maximum amount of energy is transferred (22 MBTU/min) from the oil to the coolant, shown in Figure 5.3. Thus, the oil temperature exiting the oil cooler is at a minimum of 134^{0}F. As the ambient temperature reaches a maximum of 100^{0}F, the fin-fan coolant outlet temperature reaches a maximum of 132^{0}F. At this point, 40 % less energy can be removed from the oil in the oil cooler and results in an increased oil outlet temperature of 145^{0}F.

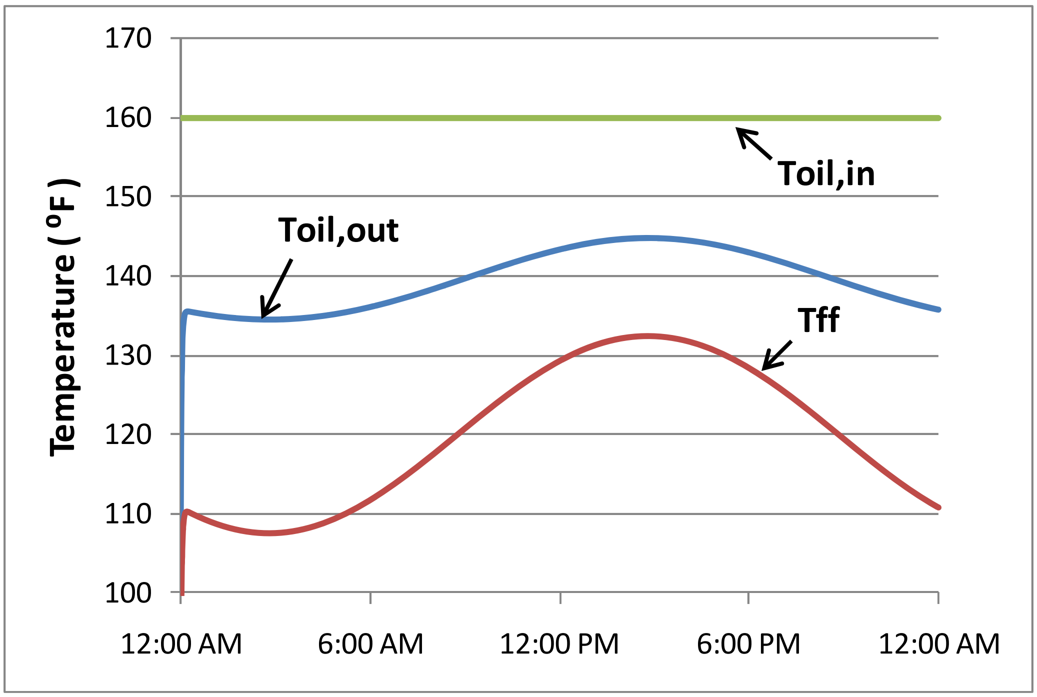

Figure 5.4 – Temperatures entering/exiting the Oil Cooler for System 1

Figure 5.5 illustrates how the coolant mass flow rates vary during daily operation. When the ambient air temperature is at its minimum, 75% of the coolant recirculates to the TCV. As the ambient air temperature reaches its maximum, the amount of coolant recirculated to the TCV drops to 67%. The change in flow rates is caused by the difference between the engine outlet temperature and the oil cooler outlet temperature, illustrated in Figure 5.6. At the lowest ambient air temperature, the temperature difference is at a maximum of 41^{0}F and as the ambient air temperature rises the temperature difference reaches a minimum of 28^{0}F. This leads to the conclusion that the ambient conditions have an impact on the energy transferred to and from the system and the resulting temperatures throughout the system.

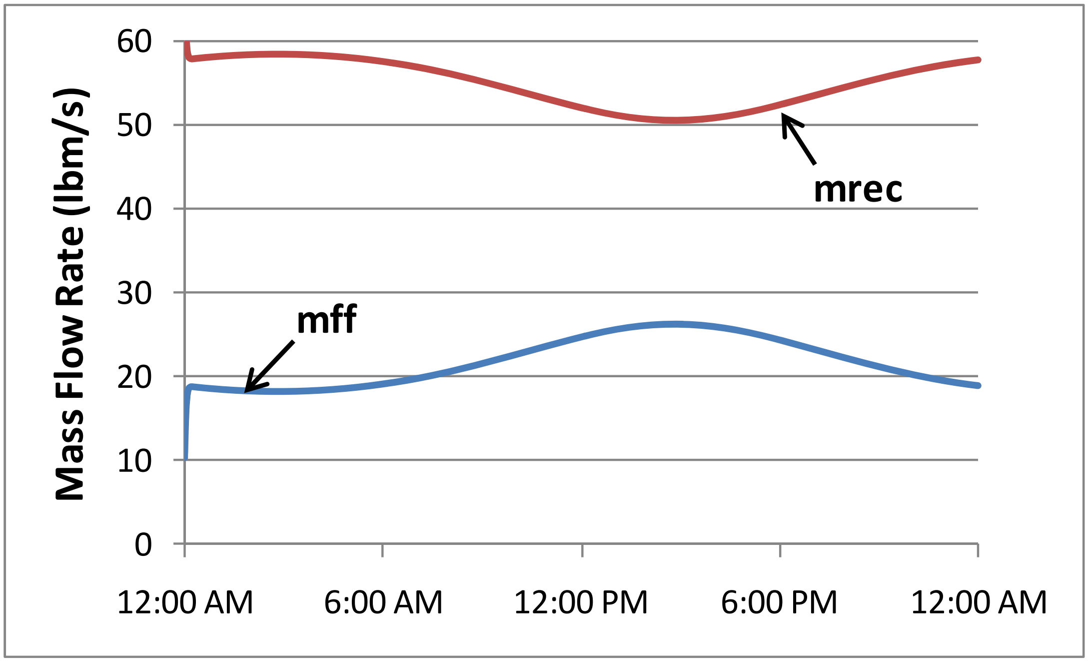

Figure 5.5 – System 1 Mass Flow Rates for System 1

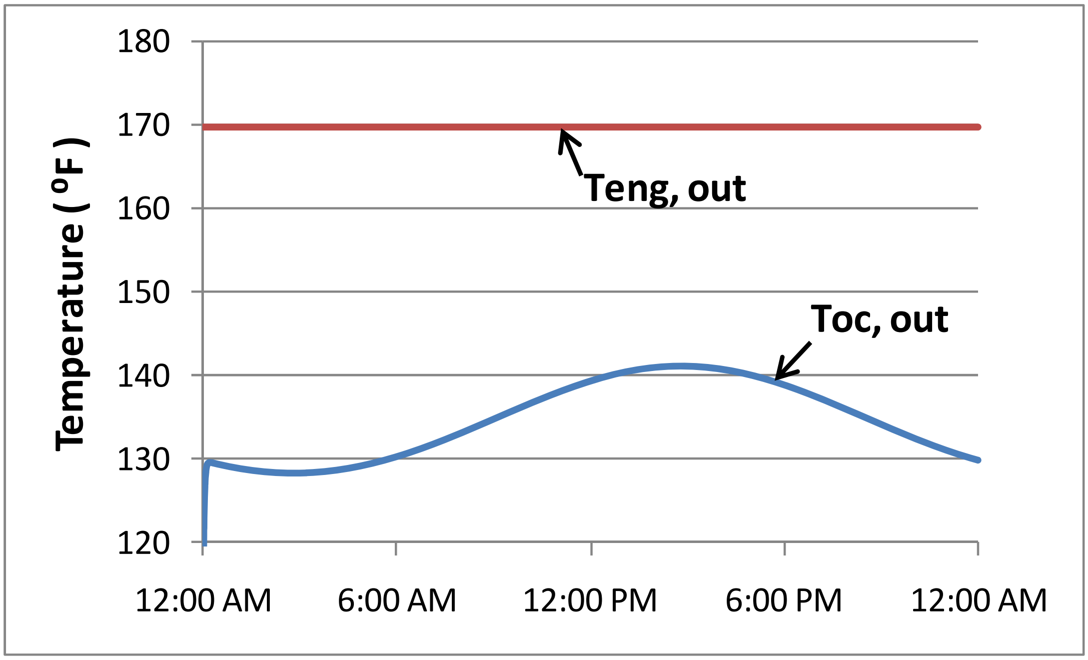

Figure 5.6 – Engine Coolant and Oil Cooler Coolant Outlet Temperature for System 1

5.2 Ambient Conditions and System 2

System 2, shown in Figure 5.7, is a dual circuit cooling system consisting of an engine jacket water cooling side and an auxiliary cooling side. On the jacket water side, the TCV controls the temperature into the engine; and, on the auxiliary cooling side, a second TCV controls the temperature into the aftercooler. Since the temperature into the engine is set by the TCV, the heat transfer rate and coolant temperature from the engine will be constant in the jacket water side. On the auxiliary cooling side, the air entering the aftercooler will increase as the ambient air temperature increases. Figure 5.8 shows how the heat transfer rates from the aftercooler and the oil cooler to the coolant vary with the changing ambient temperature. As the ambient temperature approaches its maximum of 100°F, the temperature of the air entering the aftercooler also increases. This leads to an increase in heat transfer from the air to the coolant, illustrated in Figure 5.8, and a higher coolant outlet temperature. The coolant enters oil cooler where the heat transfer rate from the oil to the coolant is reduced due to the higher coolant temperature.

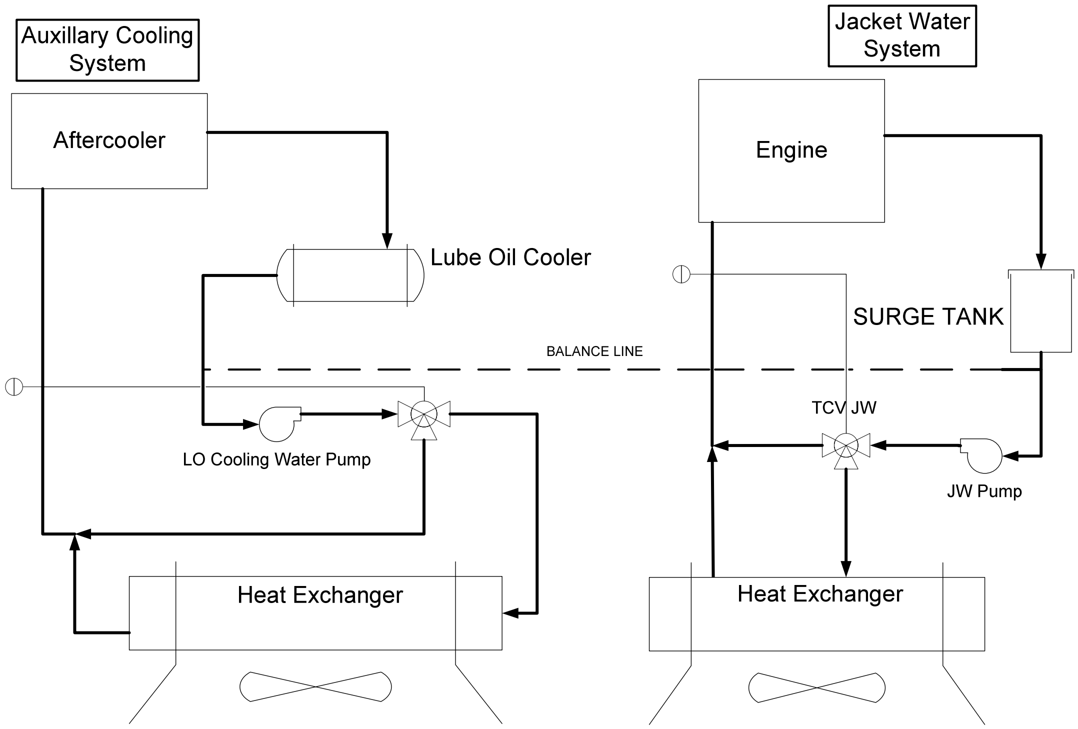

Figure 5.7 – Layout of System 2

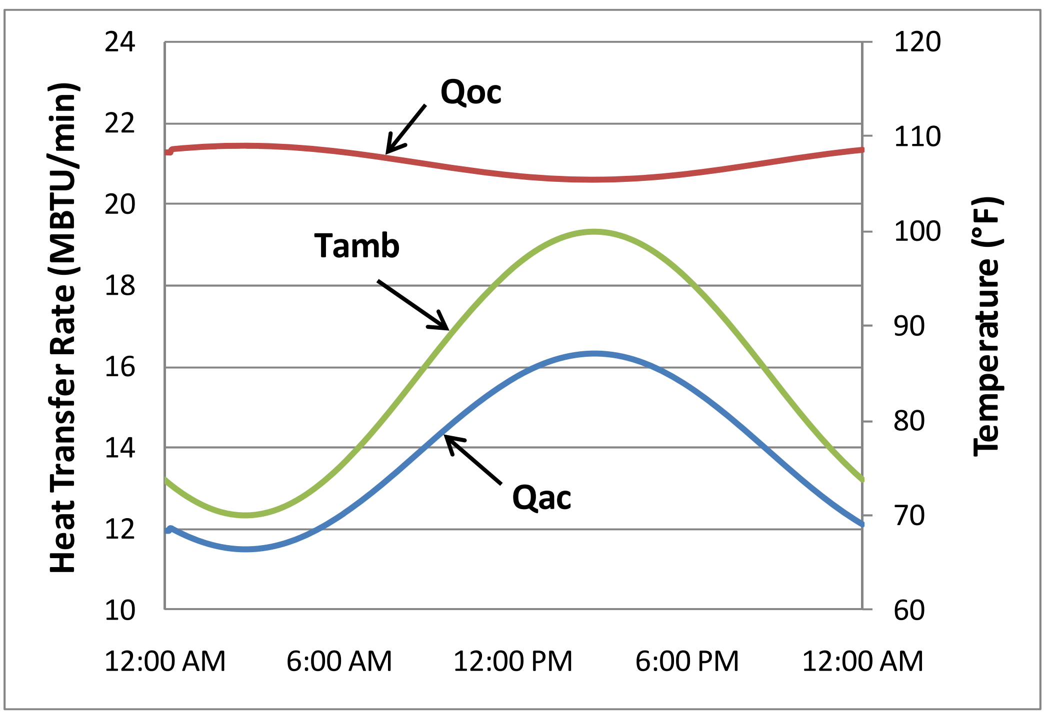

Figure 5.8 – Auxiliary Cooling System Heat Transfer Rates for System 2

The mass flow rate of the coolant into the fin-fan unit must vary in order to account for the changes in ambient conditions. Figures 5.9 and 5.10 show how the mass flow rates change with the ambient temperature for the auxiliary cooling side and the engine cooling side, respectively. In both figures, the mass flow rates behave in the same manner as discussed in Section 5.1. For the auxiliary cooling side, in Figure 5.9, the mass flow rate of the coolant into the fin-fan unit becomes larger than the recirculating mass flow rate at high ambient temperatures. This is due to the lower total mass flow rate (350 GPM) in the auxiliary cooling side.

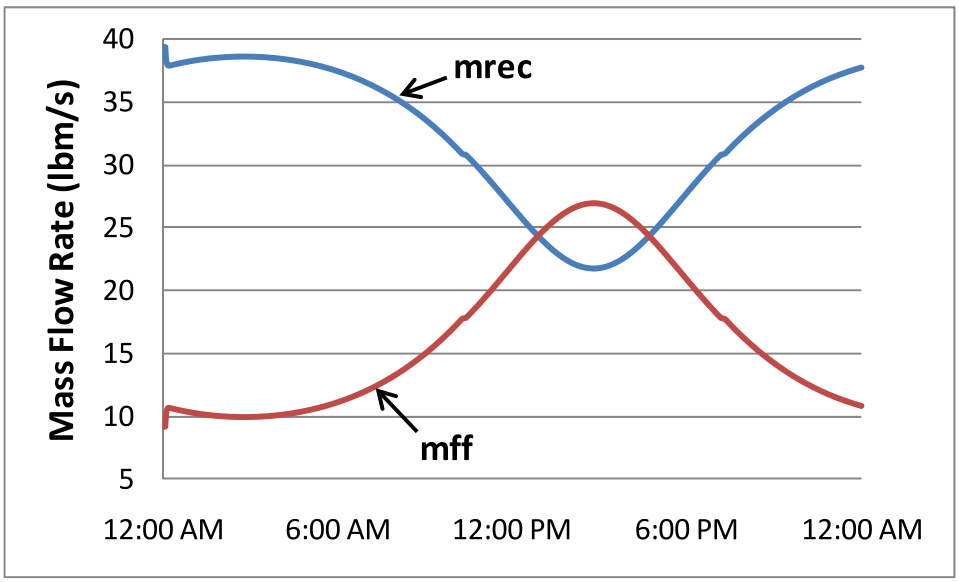

Figure 5.9 – Auxiliary Cooling Side Mass Flow Rates for System 2

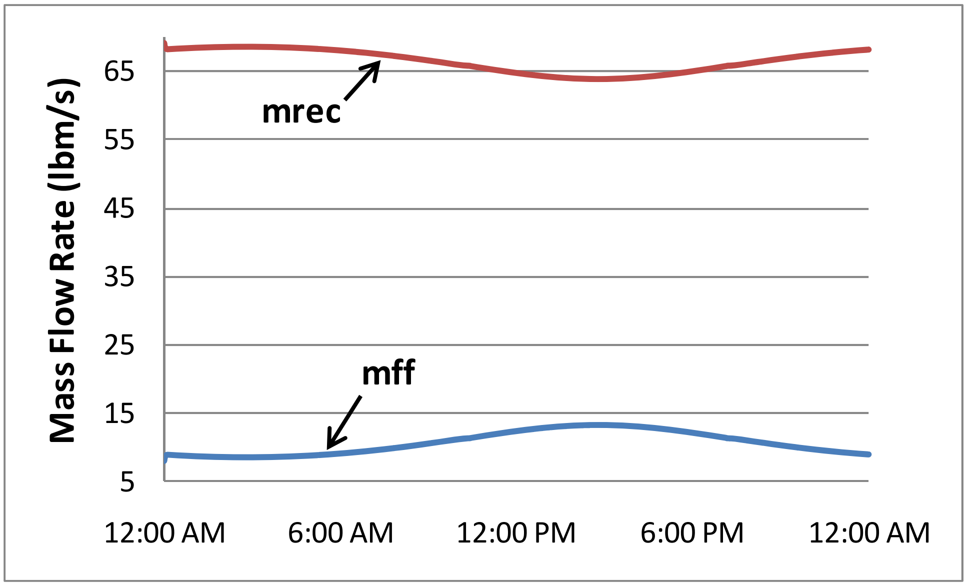

Figure 5.10 – Engine Jacket Water Side Mass Flow Rates for System 2

Other components to be considered with system 2 are the inlet and outlet conditions of the air in the aftercooler. The air from the turbocharger enters the aftercooler at a temperature that is dependent upon the turbocharger efficiency and the pressure ratio. As the pressure ratio increases, the temperature exiting the turbocharger increases. Figure 5.11 shows the resulting heat transfer from the aftercooler to the coolant versus pressure ratio. The outlet temperature of the air from the aftercooler is set at 120°F. Figure 5.11 shows that the heat transfer rate increases as the pressure ratio increases from 1.4 to 2.3. The increase in the heat transfer rate in the aftercooler results in a higher coolant outlet temperature. The higher coolant temperature leads to a reduction in heat transfer in the oil cooler due to the decreased temperature differential between oil and coolant entering the oil cooler.

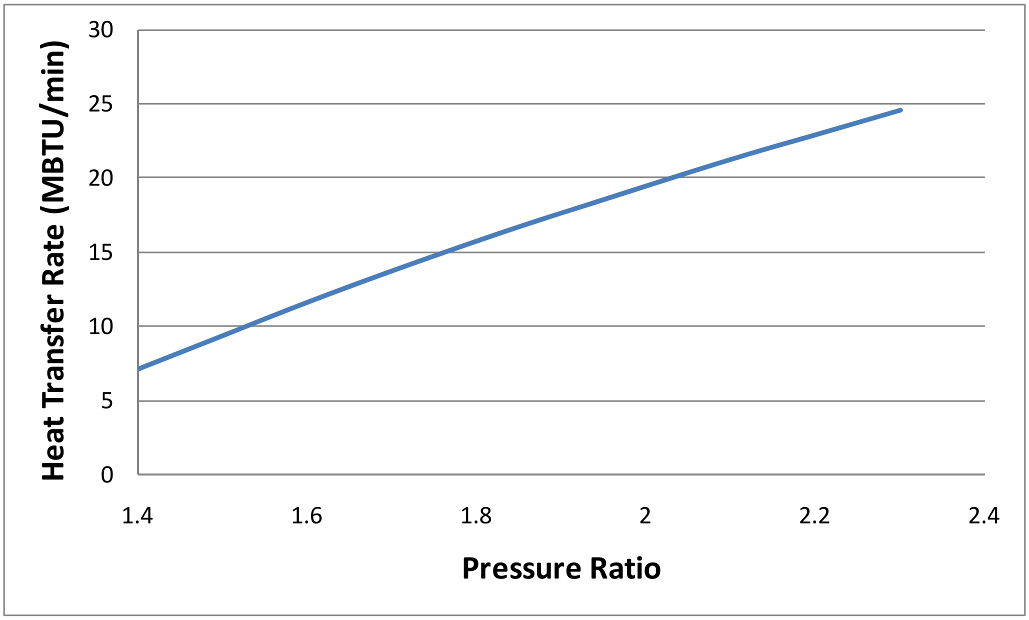

Figure 5.11 – Heat Transfer from Aftercooler vs. Pressure Ratio for System 2

5.3 Variable engine speed

Integrated into the cooling system model is a variable engine speed model. The variable engine speed model allows the user to see how the cooling system in question responds as the engine speed is ramped up to full speed. When the engine speed is changed, the cooling system model determines the resulting changes in pump head, coolant flow rate, heat transfer from the engine, and cooling equipment pressure differentials. Table 5.4 shows the calculated values for the above mentioned variables at full speed and part speed for system 1.

Table 5.4 – System 1 Parameters at Full and Part Speed for System 1

	330 RPM	200 RPM
H_p (ft)	65.0	23.3
$\dot{m}_{pump}$ (lbm/s)	75.0	45.6
q_{eng} (BTU/min)	48623.0	42310.6
Δp_{eng} (psi)	12.0	5.0
Δp_{finfin} (psi)	10.0	3.5
$\Delta p_{oilcooler}$ (psi)	10.0	3.5

Figure 5.12 shows the heat transfer rate from the engine to the coolant and from the fin-fan unit to the environs as the engine speed varies from 75% to 100%. As the speed increases from 75% to 100%, the heat transfer rates increase by 10%.

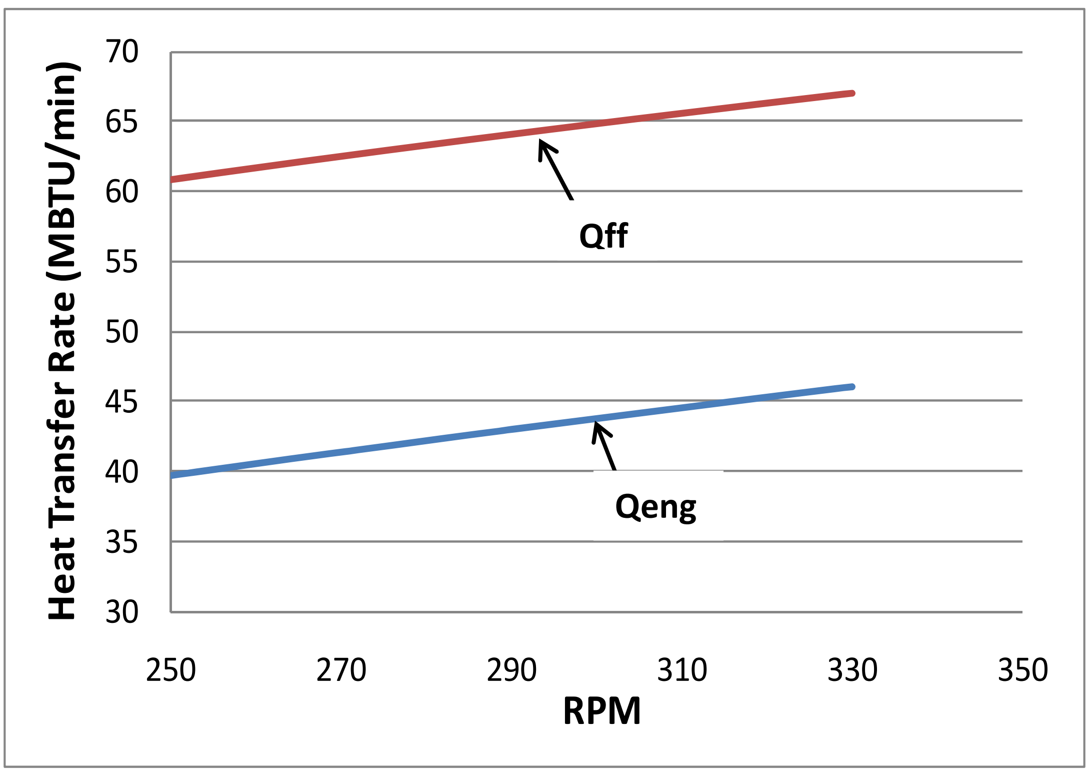

Figure 5.12 – Heat Transfer Rates vs. RPM for System 1

Modifying the engine speed causes a domino effect within the cooling system. The effect is explained as:

1. The engine speed affects the coolant pump speed and the heat transferred to the coolant from the engine.
2. The pump speed produces the head and mass flow rate in the system.
3. The mass flow rate dictates the pressure differentials within the cooling equipment.
4. The pump head and pressure differentials dictate the pressures throughout the cooling system.
5. The heat transferred from the engine, along with the ambient temperature, affects the temperatures within the cooling system.

5.4 Variable Engine Torque

By varying the fuel flow rate into the engine, users can also vary the torque on the engine at a specified speed. Since the engine speed governs the total coolant flow rate and the pump head, varying torque will not affect these cooling system parameters. Figure 5.13 shows the resulting heat transfer rates from the engine to the coolant for 75%-100% load. It is seen in Figure 5.13 that as the engine load increases, so does the heat transfer rates. Figure 5.14 shows the heat transfer rate from the fin-fan unit for 75%-100% load. It is seen, again, as the load increases, more heat is added to the cooling system and, thus, must be removed by the fin-fan unit.

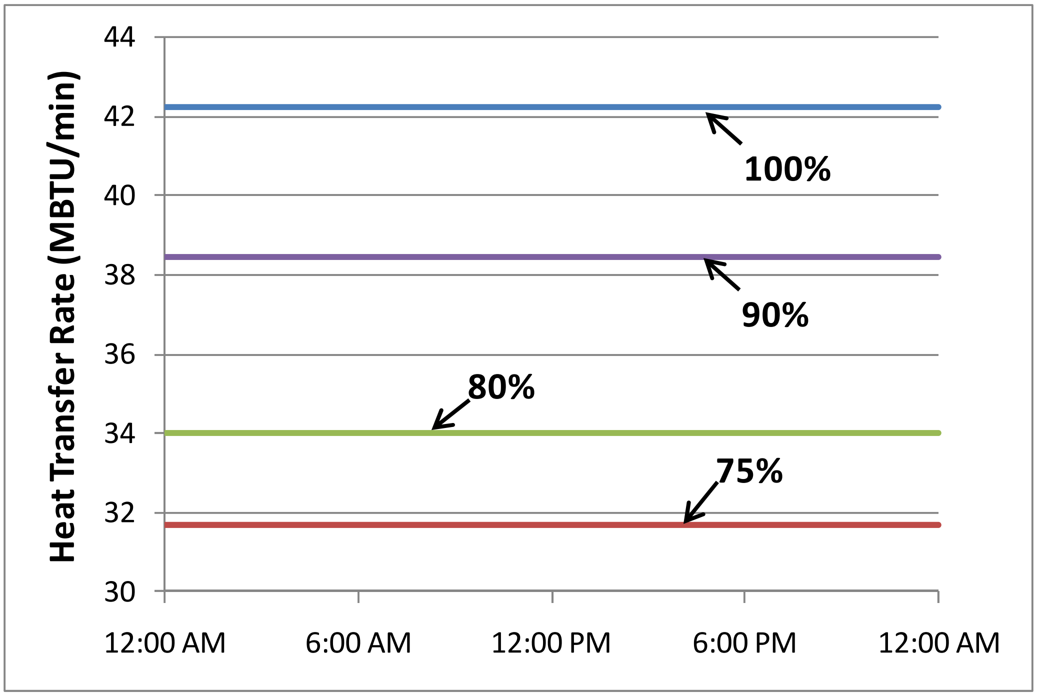

Figure 5.13 – Heat Transfer from Engine at Various Loads for System 1

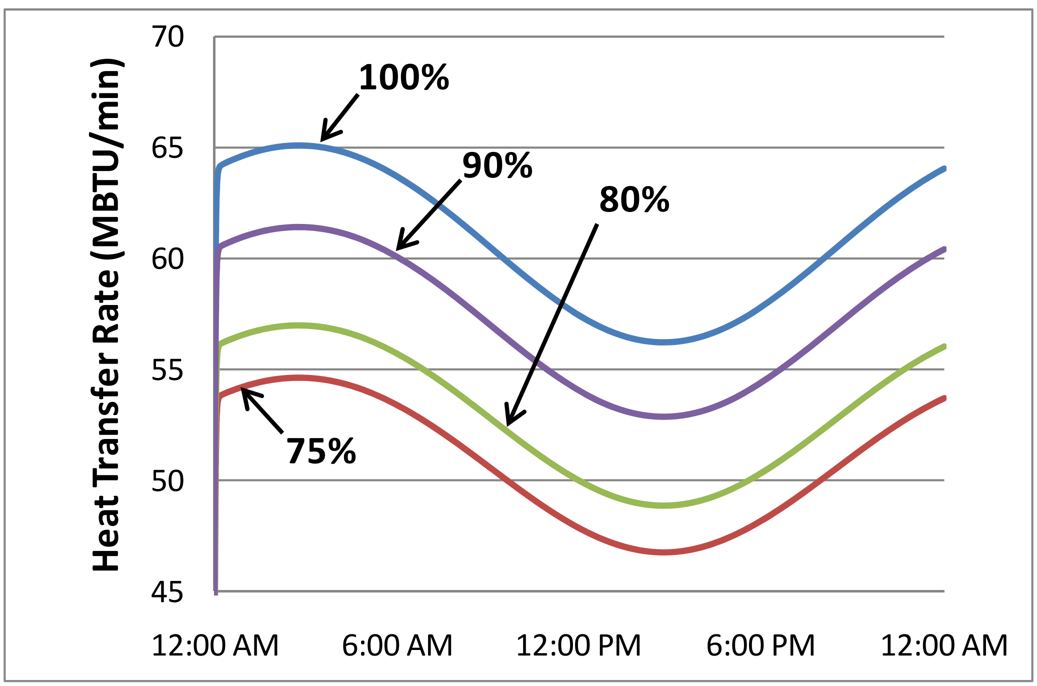

Figure 5.14 – Heat Transfer from the Fin-Fan Unit at Various Loads for System 1

5.5 Cooling System Guidelines Discussion

As discussed in the introduction, the developed cooling system guidelines represent the thesis and consist of all modeling equations, the cooling system logic tree, detailed literature and information review, and instructions on how to use the cooling system model and logic tree. The fluid dynamic, thermodynamic, and heat transfer equations used to develop the model have been thoroughly discussed in the previous sections of this thesis. Let us now look at the other components that make up the cooling system guidelines.

The cooling system logic tree was developed to help operators understand and troubleshoot cooling systems. The logic tree is built into excel and works in conjunct with the developed cooling system model. The cooling system problems addressed by the logic tree are:

1. Fouling in the components
2. Leaks throughout the system
3. Pump issues
4. Coolant and lube oil thermostatic control valve problems
5. Fin-Fan unit problems

During the literature review conducted in Task 1, OEM operating guides were collected for the engines in the focus group. Information concerning engine parameters were taken from the OEM guide and summarized in tables for convenience. These tables are included in Appendix A of this thesis.

Chapter 6 - Conclusion

A logic tree was developed as part of the PRCI funded project to assist operators in understanding cooling systems and finding possible problems within the cooling system. To supplement the logic tree, an engine cooling system modeling program has been developed for large bore two-stroke cycles engines. The model governing equations are based upon the fluid dynamics, thermodynamics, and heat transfer experienced within the cooling system. The input parameters are familiar to the operators and include engine characteristics, piping system characteristics, ambient conditions, coolant chemistry, and engine oil system characteristics. The cooling system model is an Excel-based model that relies on the embedded FORTRAN code and T-RECS program to perform the necessary calculations. The conclusions drawn from this model are:

- Since the pump head and flow rate are governed by the engine speed, the engine speed dictates the engine coolant inlet pressure and mass flow rate.
- The model calculated values are within 10% of the field collected data.
- The model can be:
    - Used to properly size cooling system components.
    - Tuned to fit actual cooling system data.
    - Used by operating companies to determine if the cooling equipment within the system is able to handle the heat loads experienced during daily operation.
- The system model is able to analyze a cooling system when the engine is not operating at full speed and as the engine ramps up to full speed.

The recommendations for future work are:

- In order to further validate the cooling system model, the model should be field tested against data collected throughout an entire system.
- To get full use of the cooling system model, more instrumentation should be incorporated into cooling systems.
- Develop a lube oil system model that is directly incorporated into the cooling water system model.

- Extend the cooling system model to encapsulate other cooling system layouts such as a common cooling system for multiple engines and variable fan speeds.
- Investigate the benefits of implementing true variable speed cooling water pumps versus cost/downfalls.

References

[1] K.S. Chapman. “The Enhancement and Validation of a Vehicle Engine Cooling System Simulation for Use as a Cooling System Design Tool,” M.S. thesis, ME, MTU, Houghton, MI, 1987.

[2] K.S. Chapman, E. Chiang, and J.H. Johnson, “The Use of the Vehicle Engine Cooling System Simulation as a Cooling System Design Tool,” SAE Congress and Symposium, 880600, Detroit, MI, 1988.

[3] B. J. Luptowski, O. Arici, J.H. Johnson, G.G. Parker, “Development of enhanced vehicle and engine cooling system simulation and application to active cooling control”. in *SAE World Congress*, pp. 197–210, Detroit, MI, USA, April 2005.

[4] K. Robinson, J.G. Hawley, N.A.F. Campbell, and D.G. Tilley, “A review of precision engine cooling,” in *International Congress and Exposition*, Detroit, Mich., 1999.

[5] W.M. Kays, “Heat transmission from the engine to the atmosphere,” *Proceedings of the International Centre for Heat and Mass Transfer*, pp. 333, 1989.

[6] M.J. Moran, H.N. Shapiro, *Fundamentals of Engineering Thermodynamics*, John Wiley, Hoboken, NJ 2007.

[7] W.F Stoecker. *Design of Thermal Systems*. New York: McGraw-Hill, 1989, pp. 80-152.

[8] S.V. Patankar, *Numerical Heat Transfer and Fluid Flow*, Hemisphere, Washington, D.C., 1980.

[9] F.P. Incropera, D.P. DeWitt, T.L. Bergman, A.S. Lavine, *Fundamentals of Heat and Mass Transfer*, John Wiley, Hoboken, NJ 2007.

[10] M.I. Karamangil, O. Kaynakli, A. Surmen, Parametric investigation of cylinder and jacket side convective heat transfer coefficients of gasoline engines. *Energy conversion and management*, vol. 47, no. 6, pp. 800, April 2006.

[11] W. J. D. Annand, "Heat Transfer in the Cylinders of Reciprocating Internal Combustion Engines," *Proc. Inst. Mech. Eng*., vol. 177, no. 36, 1963.

[12] G. Woschni, "A Universally Applicable Equation for the Instantaneous Heat Transfer Coefficient in the Internal Combustion Engine," SAE Paper 670931, 1967.

[13] Chapman, K.S and Keshavarz, A., 2002, "Development of Turbocharger-Reciprocating Engine Compressor Simulation (T-RECS)," Final Report, Gas Technology Institute, 8111.

[14] National Bureau of Standards, 1971, "JANAF Thermodynamic Tables," Publication NSRDS-NBS37.

[15] J. W. Daily and D. R. F. Harleman. "Nonuniform Flow in Conduits" in *Fluid Dynamics*. Reading, MA: Addison-Wesley Pub. Co., 1966, pp. 309-327.

[16] C. T. Crowe, D. F. Elger, and J. A. Roberson. "Flow in Conduits" in *Engineering Fluid Mechanics*, 8th ed., John Wiley & Sons, 2005, pp. 368-418.

[17] F.C. McQuiston, J.D. Parker, J.D. Spitler, *Heat, Ventilating, and Air Conditioning: Analysis and Design*, John Wiley, Hoboken, NJ, 2005.

[18] Fluide Design Inc., http://www.pumpfundamentals.com/images/tutorial/friction%20loss-fitting.pdf, Retrieved (September 2010)

[19] M. Sullivan, *Precalculus*, Prenctice Hall, Upper Saddle River, NJ, 2002.

[20] R. Wachowiak, “Jacket Water PCRI09-002 Data.xls,” Personal E-mail (July 22, 2010).

Appendix A - OEM Operating Data

Table A.1 – Cooper Bessemer Engines

Copper-Bessemer Cooling System	V - 250	V - 275	W-330	GMVA	GMVA-A	GMVE	GMVH
Coolant Temperature Exiting Engine (a)	160°F-170°F	160°F-170°F	160°F-170°F	160°F-170°F	160°F-170°F	160°F-170°F	160°F-170°F
Max Coolant Temperature Rises Across Engine (a)	10°F	10°F	10°F	10°F	10°F	10°F	10°F
Coolant Δp Through Oil Cooler *(psi)*	12	12	12	Need Data	Need Data	Need Data	12
Coolant Temperature Entering Oil Cooler	Need Data	Need Data	Need Data	115°F	115°F	115°F	115°F
Coolant Temperature Exiting Oil Cooler	Need Data	Need Data	Need Data	125°F	125°F	125°F	125°F
Jacket Water Δp *(psi)*							
4-Cylinder	n/a	n/a	n/a	10	10	10	10
6-Cylinder	6	6	n/a	10	10	10	10
8-Cylinder	7	7	10	10	10	10	10
10-Cylinder	9	9	10	10	10	10	10
12-Cylinder	11	11	18	10	10	10	10
14-Cylinder	13	13	18	n/a	n/a	n/a	n/a
16-Cylinder	15	15	18	n/a	n/a	n/a	n/a
Jacket Water Capacity *(Gal.)*							
4-Cylinder	n/a	n/a	n/a	136	n-a	n-a	n-a
6-Cylinder	480	480	n/a	204	204	204	204
8-Cylinder	615	615	615	272	272	272	272
10-Cylinder	750	750	750	340	340	340	340
12-Cylinder	890	890	890	408	408	408	480
14-Cylinder	1020	1020	1020	n/a	n/a	n/a	n/a
16-Cylinder	1160	1160	1160	n/a	n/a	n/a	n/a
Coolant Through Engine Jackets And Pump Head *(GPM - TDH)*							
4-Cylinder	n/a	n/a	n/a	130 - 81'	n-a	n-a	n-a
6-Cylinder	430 - 76'	521 - 85'	n/a	195 - 81'	216 - 81'	240 - 81'	280 - 68'
8-Cylinder	595 - 72'	694 - 80'	750 - 95'	265 - 80'	288 - 80'	317 - 80'	373 - 67'
10-Cylinder	750 - 84'	868 - 92'	940 - 85'	325 - 80'	360 - 80'	401 - 80'	468 - 66'
12-Cylinder	880 - 76'	1085 - 82'	1130 - 72'	375 - 80'	432 - 80'	480 - 80'	560 - 65'
14-Cylinder	1030 - 82'	1248 - 86'	1315 - 65'	n/a	n/a	n/a	n/a
16-Cylinder	1206 - 76'	1432 - 85'	1500 - 89'	n/a	n/a	n/a	n/a
Manifold Air Cooler Δp *(psi)*							
4-Cylinder	n/a	n/a	n/a	Not Turbocharged	n/a	n/a	n/a
6-Cylinder	3	3	n/a	Not Turbocharged	Not Turbocharged	Not Turbocharged	4
8-Cylinder	3	3	5	Not Turbocharged	Not Turbocharged	Not Turbocharged	4
10-Cylinder	5	5	5	Not Turbocharged	Not Turbocharged	Not Turbocharged	4
12-Cylinder	7	7	7	Not Turbocharged	Not Turbocharged	Not Turbocharged	4
14-Cylinder	7	7	7	n/a	n/a	n/a	n/a
16-Cylinder	7	7	7	n/a	n/a	n/a	n/a
Manifold Air Cooler Coolant Flowrate *(GPM each)*							
4-Cylinder	n/a	n/a	n/a	Not Turbocharged	n/a	n/a	n/a
6-Cylinder	8	8	n/a	Not Turbocharged	Not Turbocharged	Not Turbocharged	75
8-Cylinder	8	8	10	Not Turbocharged	Not Turbocharged	Not Turbocharged	75
10-Cylinder	10	10	10	Not Turbocharged	Not Turbocharged	Not Turbocharged	100
12-Cylinder	12	12	12	Not Turbocharged	Not Turbocharged	Not Turbocharged	100
14-Cylinder	12	12	12	n/a	n/a	n/a	n/a
16-Cylinder	12	12	12	n/a	n/a	n/a	n/a
Cooling Water System Flow and Pump Head *(GPM - TDH)*							
4-Cylinder	n/a	n/a	n/a	Not Turbocharged	n/a	n/a	n/a
6-Cylinder	250 - 60'	250 - 60'	n/a	Not Turbocharged	Not Turbocharged	Not Turbocharged	280 - 51'
8-Cylinder	250 - 60'	250 - 60'	300 - 80'	Not Turbocharged	Not Turbocharged	Not Turbocharged	280 - 51'
10-Cylinder	250 - 60'	250 - 60'	300 - 80'	Not Turbocharged	Not Turbocharged	Not Turbocharged	350 - 44'
12-Cylinder	300 - 58'	300 - 58'	350 - 78'	Not Turbocharged	Not Turbocharged	Not Turbocharged	350 - 44'
14-Cylinder	300 - 58'	300 - 58'	350 - 78'	n/a	n/a	n/a	n/a
16-Cylinder	350 - 57'	351 - 57'	350 - 78'	n/a	n/a	n/a	n/a

Copper-Bessemer Lube Oil System	V - 250	V - 275	W-330	GMVA	GMVA-A	GMVE	GMVH
Oil Temperature Exiting Engine	165°F - 170°F	165°F - 170°F	165°F - 170°F	165°F - 170°F	165°F - 170°F	165°F - 170°F	165°F - 170°F
Oil Pressure *(psi)*	25 - 30	26 - 30	40 - 50	18 - 25	19 - 25	20 - 25	21 - 25
Max Oil Temperature Rises Across Engine	10°F	10°F	10°F	10°F	10°F	10°F	10°F
Oil Filter Δp *(psi)*	4	4	4	4	4	4	4
Oil Strainer Δp *(psi)*	4	4	4	4	4	4	4
Oil Crankcase Capacity *(Gal.)*							
4-Cylinder	n/a	n/a	n/a	85	n/a	n/a	n/a
6-Cylinder	250	250	n/a	140	140	140	140
8-Cylinder	310	310	310	195	195	195	195
10-Cylinder	380	380	380	250	250	250	250
12-Cylinder	439	439	439	300	300	300	300
14-Cylinder	500	500	500	n/a	n/a	n/a	n/a
16-Cylinder	563	563	563	n/a	n/a	n/a	n/a
Oil Pump Capacity *(GPM)*							
4-Cylinder	n/a	n/a	n/a	190	n-a	n-a	n-a
6-Cylinder	300	330	n/a	190	209	209	210
8-Cylinder	419	460	396	190	209	209	210
10-Cylinder	500	550	528	274	301	301	300
12-Cylinder	500	550	528	274	301	301	300
14-Cylinder	600	660	660	n/a	n/a	n/a	n/a
16-Cylinder	600	660	750	n/a	n/a	n/a	n/a

(a) J. Sargent. "FW: 0.PRC09-002: Cooling Water Optimization Data" Personal E-mail (Aug. 9, 2009).
All other data comes from Cameron's Copper-Bessemer Engine Schematics

Table A.2 – Clark Engines

Clark Cooling System	TLA (a)	TCV (b)	HBA (c)
Coolant Temperature Entering Engine	155°F	155°F	155°F
Coolant Temperature Exiting Engine	165°F	165°F	165°F
Max Coolant Temperature Rises Across Engine	10°F	10°F	10°F
Coolant Temperature to Scavenging Air Cooler	120°F	120°F	Need Data
Jacket Water Capacity *(Gal.)*			
5-Cylinder	490	Need Data	Need Data
6-Cylinder	585	Need Data	Need Data
8-Cylinder	780	Need Data	Need Data
10-Cylinder	975	1050	Need Data
12-Cylinder	n/a	1250	Need Data
16-Cylinder	n/a	1650	Need Data
Coolant Through Engine Jackets And Break Horsepower *(GPM - BHP)*			
5-Cylinder	Need Data	Need Data	Need Data
6-Cylinder	Need Data	Need Data	Need Data
8-Cylinder	Need Data	Need Data	Need Data
10-Cylinder	860 - 3400 (d)	Need Data	1164 - 2200 (d)
12-Cylinder	Need Data	Need Data	Need Data
16-Cylinder	Need Data	1328 - 5500 (d)	Need Data
Max Temperature Rise Through Scavening Air Cooler			
Internal Cooler	17.5°F	n/a	n/a
External Cooler	6.5°F	6.5°F	n/a
Scavening Air Cooler Coolant Flow *(GPM)*			External
5-Cylinder	50	Need Data	110
6-Cylinder	180	Need Data	130
8-Cylinder	240	Need Data	175
10-Cylinder	330	300	220
12-Cylinder	Need Data	360	Need Data
16-Cylinder	Need Data	480	Need Data

Clark Lube Oil System	TLA (a)	TCV (b)	HBA (c)
Oil Temperature Entering Engine	145°F	145°F	145°F
Oil Temperature Entering Oil Cooler	160°F	Need Data	Need Data
Oil Temperature Leaving Oil Cooler	145°F	Need Data	Need Data
Oil Flow Rate *(GPM)*			
5-Cylinder	378	Need Data	Need Data
6-Cylinder	378	Need Data	Need Data
8-Cylinder	438	Need Data	Need Data
10-Cylinder	547	550	Need Data
12-Cylinder	n/a	550	Need Data
16-Cylinder	n/a	720	Need Data
Oil Crankcase Capacity *(Gal.)*			
5-Cylinder	250	Need Data	Need Data
6-Cylinder	300	Need Data	Need Data
8-Cylinder	350	Need Data	Need Data
10-Cylinder	450	725	Need Data
12-Cylinder	Need Data	850	Need Data
16-Cylinder	Need Data	1100	Need Data
Off-Engine Turbocharger Lubrication			
Oil Entering Cooler	165°F-195°F	165°F-195°F	Need Data
Oil Leaving Cooler	135°F	135°F	Need Data
Oil Pump Flowrate	4-7 GPM	4-7 GPM	Need Data

(a) TLA, 1st ed., Clark, Olean, NY, 1965, pp. 197-199.
(b) TCV, 1st ed., Clark, Olean, NY, 1968, pp. 211-212.
(c) Gas and Compressor Field Service Manual, Dresser-Rand Engine Process Compressor Div., Painted Post, NY, 1965, sec. 5, pp. 3 & 4a.
(d) J. Stanley. "FW: JW 50/50 coolant flow rates" Personal E-mail (Jun. 24, 2009).

Table A.3 – Ingersoll-Rand Engines

KVS Cooling System

Coolant Temperature Exiting Engine	165°F - 175°F
Coolant Temperature to Oil Cooler	110°F - 115°F
Max Coolant Temperature Rises Across Engine	12°F
Water Pump Discharge Pressure	30 -35 psi
Engine Jacket Water Pressure (Max)	50 psi
Jacket Water Flow Rate and Head *(GPM - ft)*	
KVS 26	336 - 21'
KVS 36	336 - 21'
KVS 48	448 - 21'
KVS 410	560 - 21'
KVS 412	672 - 21'
KVS 512	672 - 21'
Coolant Flow Rate to Oil Cooler and Head *(GPM - ft)*	
KVS 26	50 -1.5'
KVS 36	50 -1.5'
KVS 48	67 - 3.8'
KVS 410	83 - 6'
KVS 412	100 - 9.9'
KVS 512	100 - 9.9'
Compressor Cylinder Flow Rate *(GPM)*	
KVS 26	67
KVS 36	67
KVS 48	89
KVS 410	112
KVS 412	134
KVS 512	134

KVS Lube Oil System

Oil Temperature Entering Engine	150°F - 155°F
Oil Temperature Exiting Engine	160°F - 165°F
Oil Pressure Main Bearing Oil Header	45 - 55 psi
Crankcase Capacity *(Gal.)*	
KVS 26	120
KVS 36	150
KVS 48	200
KVS 410	240
KVS 412	240
KVS 512	270
Oil Pump Capacity *(GPM)*	
KVS 26	150
KVS 36	150
KVS 48	212
KVS 410	260
KVS 412	260
KVS 512	260
Oil Through Cooler *(GPM)*	
KVS 26	145
KVS 36	145
KVS 48	205
KVS 410	250
KVS 412	250
KVS 512	250

KVS, 1st ed., Ingersoll-Rand, Painted Post, NY, 1953, pg. 5-3.